Supporting information for:

Tridentate κ³-*P,P,C* Iridium Complexes: Influence of Ligand Saturation on Intramolecular C—H Bond Activation

Mitchell J. Demchuk,[a] Joseph A. Zurakowski,[a,b] Marcus W. Drover [a,*]

*E-mail: marcus.drover@uwo.ca

[a]Department of Chemistry, Western University, 1151 Richmond Street, London, ON, N8K 3G6, Canada

[b]Department of Chemistry and Biochemistry, The University of Windsor, 401 Sunset Avenue, Windsor, ON, N9B 3P4, Canada

Experimental Section:

General Considerations. All experiments were carried out employing standard Schlenk techniques under an atmosphere of dry nitrogen employing degassed, dried solvents in a solvent purification system supplied by PPT, LLC. Non-halogenated solvents were tested with a standard purple solution of sodium benzophenone ketyl in tetrahydrofuran to confirm effective moisture removal. d_6-benzene was dried over molecular sieves and degassed by three freeze-pump-thaw cycles. Dicyclohexylborane ($HBCy_2$),[1] *tri*-tert-butyl-allyl-diphosphinoethane (t^tbape) [2] and *tri*-tert-butyl-*n*-propyldicyclohexylboranyl-diphosphinoethane (t^tbbpe) [2] were prepared using literature procedures. Other reagents were purchased from commercial vendors and used without further purification unless otherwise stated.

Physical methods. ^{1}H NMR spectra are reported in parts per million (ppm) and are referenced to residual solvent e.g., $^1H(C_6D_6)$: δ 7.16; $^{13}C(C_6D_6)$: 128.06; coupling constants are reported in Hz. $^{13}C\{^1H\}$, $^{11}B\{^1H\}$, and $^{31}P\{^1H\}$ NMR spectra were performed as proton-decoupled experiments and are reported in ppm.

Preparation of Compounds:

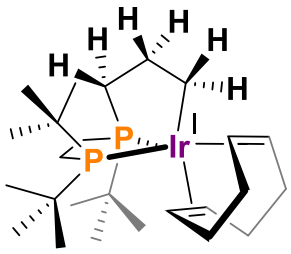

[Ir^{I}(κ^{3}-(CH$_2$)$_3$PP^{tBu}$_3$)(COD)] (**(±)-1:** $C_{25}H_{49}P_2Ir$, M_W = 603.8 g/mol): In the glovebox, [Ir(μ-OCH$_3$)(COD)]$_2$ (24 mg, 0.036 mmol, 1 equiv.) was weighed into a 20 mL scintillation vial equipped with a stir bar and dissolved in *ca*. 0.5 mL THF. Then, t^{t}bbpe (35 mg, 0.073 mmol, 2 equivs.) was dissolved in *ca*. 1 mL THF and added to the vial while mixing, immediately turning dark yellow/murky orange. This reaction was allowed to stir for 3 h, resulting in a murky dark orange solution, after which volatiles were removed *in vacuo*. The resulting orange oily solid was dissolved in pentane and filtered using Celite® (the crude yield after this step was 47 mg (107%), as side product, MeO-BCy$_2$ was still present; >96% purity *via* $^{31}P\{^1H\}$ NMR spectroscopy). Orange crystals suitable for analysis by single crystal X-Ray diffraction were grown from a minimal amount of pentane at -35 °C over the course of 3 days (more material can be obtained from subsequent crystallizations). These crystals can be quickly washed with cold pentane to remove the side product, CH$_3$OBCy$_2$ to give **(±)-1** in >99% purity *via* $^{31}P\{^1H\}$ NMR spectroscopy (18 mg, 41%). **^{1}H NMR (600 MHz, C$_6$D$_6$, 298 K):** δ_H = 4.40 (br, 1H; C**H** COD), 3.72 (br, 1H; C**H** COD), 3.16 – 2.08 (br, 10H), 2.01 (m, 2H), 1.77 (m, 2H), 1.56 (m, 1H), 1.47 (m, 1H), 1.35 (m, 2H), 1.25 (d, 9H; $^3J_{H,P}$ = 11.2 Hz; ^{t}Bu C**H**$_3$), 1.11 (d, 9H; $^3J_{H,P}$ = 11.6 Hz; ^{t}Bu C**H**$_3$), 1.01 (d, 9H; $^3J_{H,P}$ = 10.2 Hz; ^{t}Bu C**H**$_3$), 0.86 (m, 2**H**; C**H**$_2$). **^{13}C{^{1}H} NMR (151 MHz, C$_6$D$_6$, 298 K):** δ_C = 64.3 (br, **C**H COD), 62.7 (br, **C**H COD), 53.6 (br, **C**H COD), 49.6 (br, **C**H COD), 38.6 (br, **C**H$_2$ COD), 38.4 (dd, $J_{C,P}$ = 10.8, 5.5 Hz), 36.5 (br, **C**H$_2$ COD), 36.5 (dd, $J_{C,P}$ = 22.4, 7.2 Hz), 35.9 (dd, $J_{C,P}$ = 3.6, 1.1 Hz), 35.2 (dd, $J_{C,P}$ = 25.3, 5.1 Hz), 34.1 (br, **C**H$_2$ COD), 32.5 (d, $J_{C,P}$ = 4.2 Hz), 32.4 (br, **C**H$_2$ COD), 32.3 (dd, $J_{C,P}$ = 10.6, 4.7 Hz), 31.3 (d, $J_{C,P}$ = 5.00 Hz), 30.2 (dd, $J_{C,P}$ = 18.8, 15.6 Hz), 28.2 (d, $J_{C,P}$ = 5.8 Hz), 19.9 (dd, $J_{C,P}$ = 16.1, 11.7 Hz), 19.8 (dd, $J_{C,P}$ = 5.0, 3.7 Hz). **^{31}P{^{1}H} NMR (121 MHz, C$_6$D$_6$, 298 K):** δ_P = + 57.1 (d, $J_{P,P}$ = 44.5 Hz), + 53.9 (d, $J_{P,P}$ = 44.5 Hz). **HRMS (ESI):** *m*/*z* calc. for $[C_{25}H_{48}P_2Ir]^+$: 603.286 $[M-H]^+$; expt. 603.286 $[M-H]^+$. Anal. calcd for $C_{25}H_{49}P_2Ir$ (603.8): C, 49.73; H, 8.18; best found: C, 51.05; H, 8.15. These results are outside the range viewed as establishing analytical purity but are provided to illustrate the best values obtained to date. Clean NMR data indicate >95% purity

[Ir^{I}(κ^{3}-(CH)=(CH)(CH$_2$)PP$^{tBu}{}_3$)(COD)] (**(±)-2:** $C_{25}H_{47}P_2Ir$, M_W = 601.8 g/mol): In the glovebox, [Ir(μ-OCH$_3$)(COD)]$_2$ (23 mg, 0.035 mmol, 1 equiv.) was weighed into a 20 mL scintillation vial equipped with a stir bar and dissolved in *ca*. 0.5 mL THF. Then, t^{t}bape (21 mg, 0.069 mmol, 2 equivs.) was dissolved in *ca*. 1 mL THF and added to the vial while mixing, turning from yellow to cloudy dark yellow/orange. This reaction was allowed to stir for 5 minutes, resulting in an orange solution, after which volatiles were removed *in vacuo*. The resulting oily solid was dissolved in pentane and filtered using Celite® (the crude yield after this step was 29 mg (69%), with impurities *via* $^{31}P\{^{1}H\}$ NMR spectroscopy). Dark yellow crystals suitable for analysis by single crystal X-Ray diffraction were grown from a minimal amount of pentane at -35 °C over the course of 1 week (more material can be obtained from subsequent crystallizations). These crystals can be quickly washed with cold pentane to give **(±)-2** in >90% purity (**(±)-3** is the impurity) by $^{31}P\{^{1}H\}$ NMR spectroscopy (7 mg, 17%). **^{1}H NMR (600 MHz, C$_6$D$_6$, 298 K):** δ_H = 6.88 (m, 1H; $^{2}J_{H,P}$ = 47.4 Hz; P-C**H** on cyclometalated arm), 5.57 (m, 1H; $^{3}J_{H,P}$ = 12.5 Hz; C**H** middle of cyclometalated arm), 3.66 (br., 2H; C**H** COD), 3.31 (br., 2H; C**H** COD), 3.11 (m, 1H; C**H**$_2$ cyclometalated arm), 2.60 (br. m, 4H; C**H**$_2$ COD), 2.36 (br. m, 4H; C**H**$_2$ COD), 1.84 (m, 1H; *J* = 17.8 Hz; C**H**$_2$ cyclometalated arm), 1.76 – 1.38 (m, 4H, PC**H**$_2$C**H**$_2$P backbone), 1.21 (d, 9H; $^{3}J_{H,P}$ = 11.6 Hz; ^{t}Bu C**H**$_3$), 1.19 (d, 9H; $^{3}J_{H,P}$ = 12.4 Hz; ^{t}Bu C**H**$_3$), 1.05 (d, 9H; $^{3}J_{H,P}$ = 10.4 Hz; ^{t}Bu C**H**$_3$). **^{13}C{^{1}H} NMR (151 MHz, C$_6$D$_6$, 298 K):** δ_C = 163.4 (d, $J_{C,P}$ = 32.9 Hz; **C**H cyclometalated arm), 125.8 (dd, $J_{C,P}$ = 40.0, 1.8 Hz; **C**H cyclometalated arm), 57.3 (br), 55.7 (br), 37.8 (dd, $J_{C,P}$ = 9.9, 4.3 Hz), 36.3 (d, $J_{C,P}$ = 5.1 Hz), 35.3 (br), 34.8 (br), 32.5 (d, $J_{C,P}$ = 4.1 Hz), 32.1 (dd, $J_{C,P}$ = 18.0, 5.0 Hz), 31.9 (d, $J_{C,P}$ = 4.2 Hz), 31.8 (d, $J_{C,P}$ = 4.1 Hz), 31.3 (d, $J_{C,P}$ = 5.1 Hz), 29.3 (dd, $J_{C,P}$ = 20.9, 15.1 Hz), 28.3 (d, $J_{C,P}$ = 4.4 Hz), 21.7 (d, $J_{C,P}$ = 3.9 Hz), 21.4 (dd, $J_{C,P}$ = 17.3, 12.6 Hz); some resonances overlapping. **^{31}P{^{1}H} NMR (121 MHz, C$_6$D$_6$, 298 K):** δ_P = + 55.4 (d, $J_{P,P}$ = 31.6 Hz), + 46.9 (d, $J_{P,P}$ = 31.6 Hz). **HRMS (ESI):** *m*/*z* calc. for $[C_{25}H_{46}P_2Ir]^+$: 601.270 $[M-H]^+$; expt. 601.270 $[M-H]^+$. Anal. calcd for $C_{25}H_{47}P_2Ir$ (601.8): C, 49.89; H, 7.87; best found: C, 48.80; H, 7.89. These results are outside the range viewed as establishing analytical purity but are provided to illustrate the best values obtained to date. Clean NMR data indicate >95% purity

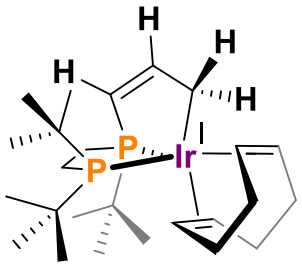

[Ir^{III}(κ^3-(CH$_2$)(CH)=(CH)PP$^{tBu}{}_3$)(1,2,3,5-η^3,η^1-C$_8$H$_{12}$)] (**(±)-3:** C$_{25}$H$_{47}$P$_2$Ir, M_W = 601.8 g/mol): In the glovebox, [Ir(μ-OCH$_3$)(COD)]$_2$ (33 mg, 0.050 mmol, 1 equiv.) was weighed into a 20 mL scintillation vial equipped with a stir bar and dissolved in *ca*. 0.5 mL THF. Next, t^{t}bape (30 mg, 0.099 mmol, 2 equivs.) was dissolved in *ca*. 1 mL THF and added to the vial while mixing, slowly going from yellow to cloudy dark yellow/orange. This reaction was allowed to stir for 24 h, resulting in a dark orange/red solution, after which volatiles were removed *in vacuo*. The resulting orange/red oily solid was dissolved in pentane and filtered using Celite® (the crude yield after this step was 47 mg (78%), with impurities *via* ^{31}P{^{1}H} NMR spectroscopy). Light orange crystals of **(±)-3** suitable for analysis by single crystal x-ray diffraction were grown from a minimal amount of pentane at -35 °C over the course of 1 week to give >99% purity *via* ^{31}P{^{1}H} NMR spectroscopy (4 mg, 7%). More material can be obtained from subsequent crystallizations. **^{1}H NMR (600 MHz, C$_6$D$_6$, 298 K):** δ_H = 8.45 (m, 1H; Ir-C**H** on cyclometalated arm), 6.13 (m, 1H; Ir-CH-C**H** on cyclometalated arm), 4.87 (m, 1H; C**H** COD), 4.69 (m, 1H; C**H** COD), 4.07 (m, 1H; C**H** COD), 3.84 (m, 1H; C**H** COD), 2.83 (m, 1H; Ir-CH-CH-C**H$_2$** on cyclometalated arm by ^{1}H-^{1}H COSY), 2.58 (m, 1H), 2.47 (m, 2H), 2.04 (m, 1H; Ir-CH-CH-C**H$_2$** on cyclometalated arm by ^{1}H-^{1}H COSY), 1.98-1.17 (m, 9H), 1.13 (d, 9H, $^3J_{H,P}$ = 12.0 Hz; ^{t}Bu C**H$_3$**), 1.08 (d, 9H, $^3J_{H,P}$ = 11.1 Hz; ^{t}Bu C**H$_3$**), 0.80 (d, 9H, $^3J_{H,P}$ = 11.0 Hz; ^{t}Bu C**H$_3$**). **^{1}H{^{31}P} NMR (600 MHz, C$_6$D$_6$, 298 K):** δ_H = 8.45 (dd, 1H; $J_{H,H}$ = 8.3 Hz, $J_{H,H}$ = 2.2 Hz; Ir-C**H** on cyclometalated arm), 6.13 (ddd, 1H; $J_{H,H}$ = 8.3 Hz, $J_{H,H}$ = 3.6 Hz, $J_{H,H}$ = 1.9 Hz; Ir-CH-C**H** on cyclometalated arm), 4.86 (m, 1H; C**H** COD), 4.69 (m, 1H; C**H** COD), 4.06 (m, 1H; C**H** COD), 3.84 (br. d, 1H; $J_{H,H}$ = 14.1 Hz; C**H** COD), 2.83 (m, 1H; Ir-CH-CH-C**H$_2$** on cyclometalated arm by ^{1}H-^{1}H COSY), 2.58 (m, 1H), 2.47 (m, 2H), 2.04 (dd, 1H; $J_{H,H}$ = 15.9 Hz, $J_{H,H}$ = 3.63 Hz; Ir-CH-CH-C**H$_2$** on cyclometalated arm by ^{1}H-^{1}H COSY), 1.91 (m, 2H), 1.76 (m, 1H), 1.65 (m, 1H), 1.45 (m, 2H), 1.36 (m, 2H), 1.26 – 1.18 (m, 4H), 1.13 (s, 9H; ^{t}Bu C**H$_3$**), 1.08 (s, 9H; ^{t}Bu C**H$_3$**), 0.70 (s, 9H; ^{t}Bu C**H$_3$**). **^{13}C{^{1}H} NMR (151 MHz, C$_6$D$_6$, 298 K):** δ_C = 143.9 (dd, $J_{C,P}$ = 5.2, 5.1 Hz; Ir-**C**H on cyclometalated arm), 121.0 (dd, $J_{C,P}$ = 14.0, 3.4 Hz; Ir-CH-**C**H on cyclometalated arm), 94.0 (d, $J_{C,P}$ = 3.6 Hz; allyl **C**H), 56.1 (d, $J_{C,P}$ = 6.2 Hz; allyl **C**H), 39.6 (d, $J_{C,P}$ = 1.7 Hz; allyl **C**H), 39.3 (d, $J_{C,P}$ = 1.7 Hz), 38.8 (dd, $J_{C,P}$ = 6.3, 2.0 Hz), 36.9 (d, $J_{C,P}$ = 6.0 Hz), 34.2 (d, $J_{C,P}$ = 5.4 Hz), 33.1 (dd, $J_{C,P}$ = 33.1, 1.3 Hz; Ir-CH-CH-**C**H$_2$), 30.9 (d, $J_{C,P}$ = 18.2 Hz), 30.8 (d, $J_{C,P}$ = 3.6 Hz), 30.0 (d, $J_{C,P}$ = 4.5 Hz), 28.4 (dd, $J_{C,P}$ = 3.4, 0.8 Hz), 27.7 (d, $J_{C,P}$ = 4.2 Hz), 27.5 (dd, $J_{C,P}$ = 27.3, 15.7 Hz), 26.0 (dd, $J_{C,P}$ = 2.1, 1.1 Hz), 25.2 (dd, $J_{C,P}$ = 4.1, 1.5 Hz), 23.5 (dd, $J_{C,P}$ = 20.4,

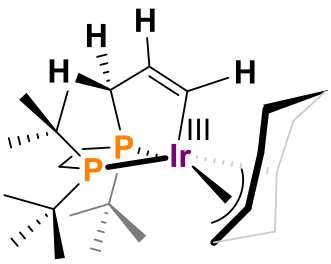

12.5 Hz). **$^{31}P\{^{1}H\}$ NMR (243 MHz, C_6D_6, 298 K):** δ_P = + 70.1 (d, $J_{P,P}$ = 2.1 Hz), + 35.5 (d, $J_{P,P}$ = 2.1 Hz). **HRMS (ESI):** *m*/*z* calc. for $[C_{25}H_{46}P_2Ir]^+$: 601.270 $[M-H]^+$; expt. 601.270 $[M-H]^+$. Anal. calcd for $C_{25}H_{47}P_2Ir$ (601.8): C, 49.89; H, 7.87; best found: C, 48.24; H, 8.07. These results are outside the range viewed as establishing analytical purity but are provided to illustrate the best values obtained to date. Clean NMR data indicate >95% purity

tri-*tert*-butyl-allyl-diphosphinoethane-d_5, (^{t}Bu)$_2$PCH$_2$CH$_2$P(^{t}Bu)(CD$_2$CDCD$_2$), t^{t}bape-d_5: $C_{17}H_{31}D_5P_2$, M_W = 307.4 g/mol): To a 100 mL two-necked Schlenk flask, was added finely cut dried magnesium turnings (96.4 mg, 3.97 mmol) and cycled onto a Schlenk line. Approximately 20 mL of dry Et$_2$O was added to the flask. A reflux condenser was attached to the top neck and a septum to the other. With vigorous stirring, allyl-bromide-d_5 (0.178 mL, 1.98 mmol) was added slowly dropwise over the course of 30 mins, without allowing the solvent to reflux. The reaction was allowed to stir for 2 h, transforming from a clear colorless solution to a colorless solution with off-white precipitate. The solution was then cannula filtered into another 100 mL Schlenk flask and the reaction vessel was washed with 5 mL of Et$_2$O. In another 200 mL pear flask, (di-*tert*-butyl-phosphino)-2-(tert-butyl-iodo-phosphino)ethane, (^{t}Bu)$_2$PCH$_2$CH$_2$P(^{t}Bu)(I) (377.6 mg, 0.972 mmol) was weighed and dissolved in 80 mL THF. The flask was cycled onto the Schlenk line and cooled to 0 °C. Using a nitrogen purged syringe, the *in-situ* prepared solution of allyl-magnesium bromide-d_5 was added slowly to the flask containing ^{t}(Bu)$_2$PCH$_2$CH$_2$P(^{t}Bu)(I), while stirring over the course of 30 mins. The reaction was then allowed to warm to room temperature and stirred for an additional 2 h (a white precipitate formed). Solvent was removed *in-vacuo* and the reaction vessel was brought into a glovebox. The dried white solid was then washed with 5 x 4 mL of pentane and filtered through a 0.1 μm PTFE syringe filter into a 20 mL scintillation vial. The solvent was removed *in-vacuo* leaving a viscous white oil (260 mg, 87%). *N.B.* this compound was 80% pure by ^{31}P{^{1}H} NMR spectroscopy and was used without further purification. The impurity is the known dimer, (^{t}Bu)$_2$PCH$_2$CH$_2$P(^{t}Bu)-P(^{t}Bu)CH$_2$CH$_2$P(^{t}Bu)$_2$.[2] ^{1}H NMR data as previously reported.[2] **^{31}P{^{1}H} NMR (243 MHz, C$_6$D$_6$, 298 K):** δ_P = + 34.8 (d, $J_{P,P}$ = 29.9 Hz), + 1.62 (d, $J_{P,P}$ = 29.9 Hz).

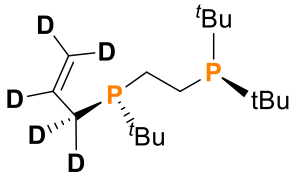

NMR Data:

Figure S1. (±)-1, ^{1}H NMR, C_6D_6, 600 MHz, 298 K.

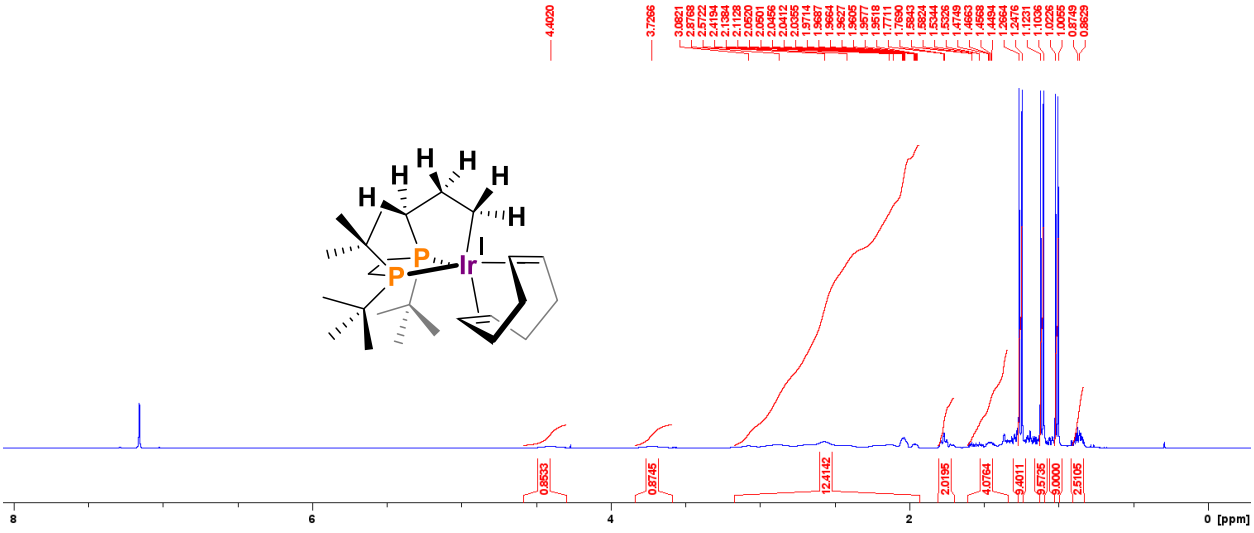

Figure S2. (±)-1, ^{1}H NMR (expansion), C_6D_6, 600 MHz, 298 K.

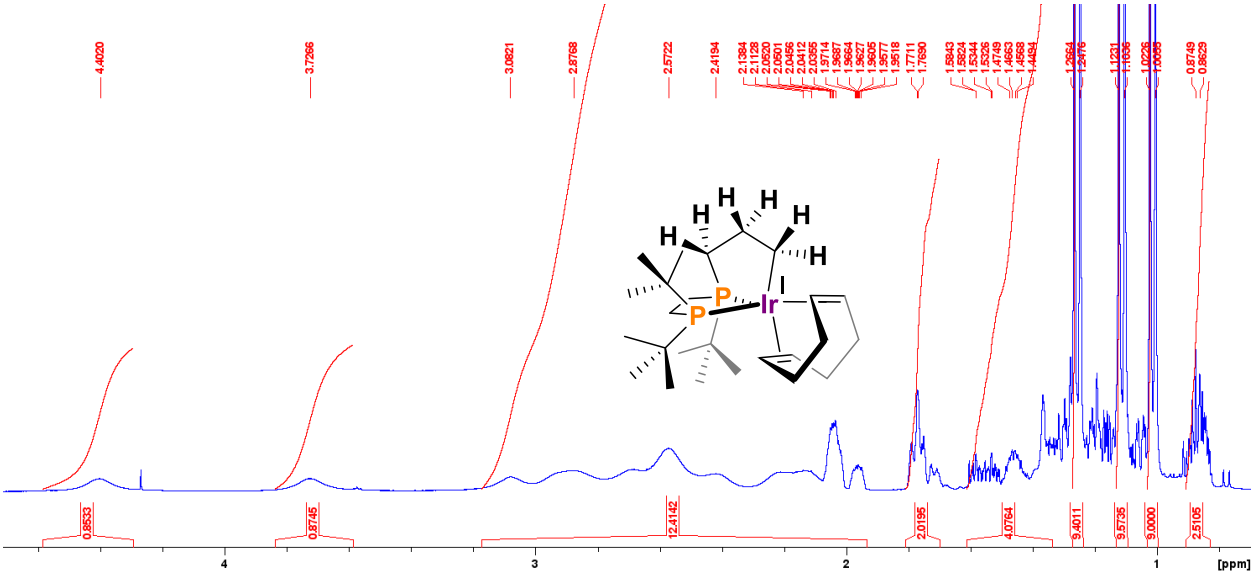

Figure S3. (±)-1, $^{1}H\{^{31}P\}$ NMR, C_6D_6, 600 MHz, 298 K.

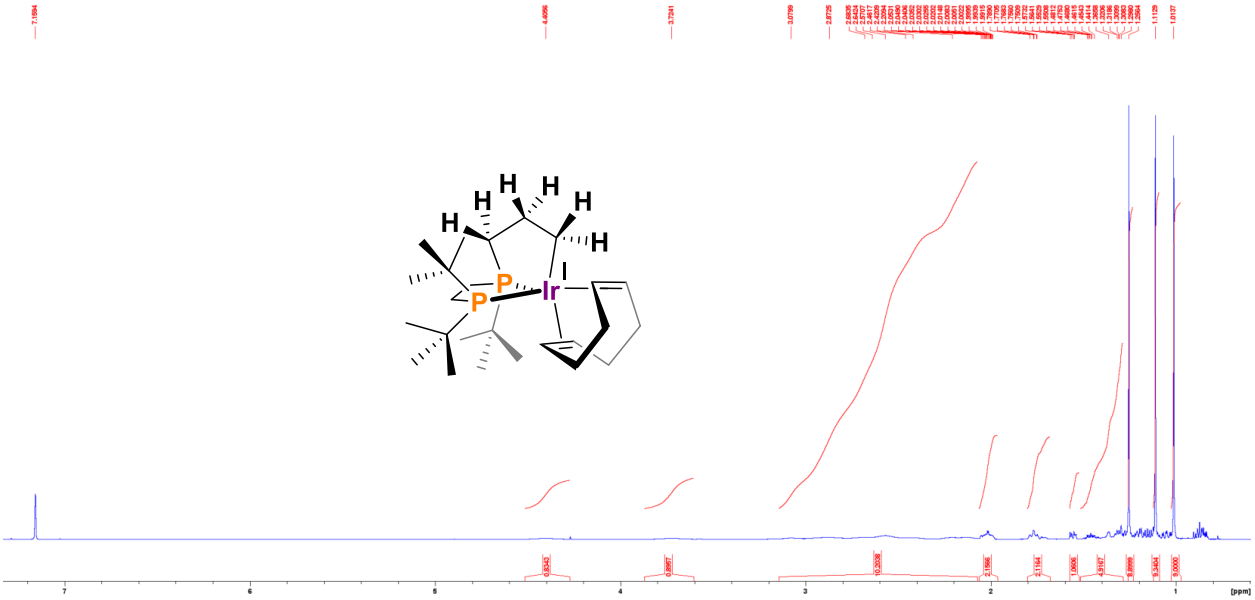

Figure S4. (±)-1, ^{1}H (blue)/$^{1}H\{^{31}P\}$ (red) NMR, C_6D_6, 600 MHz, 298 K.

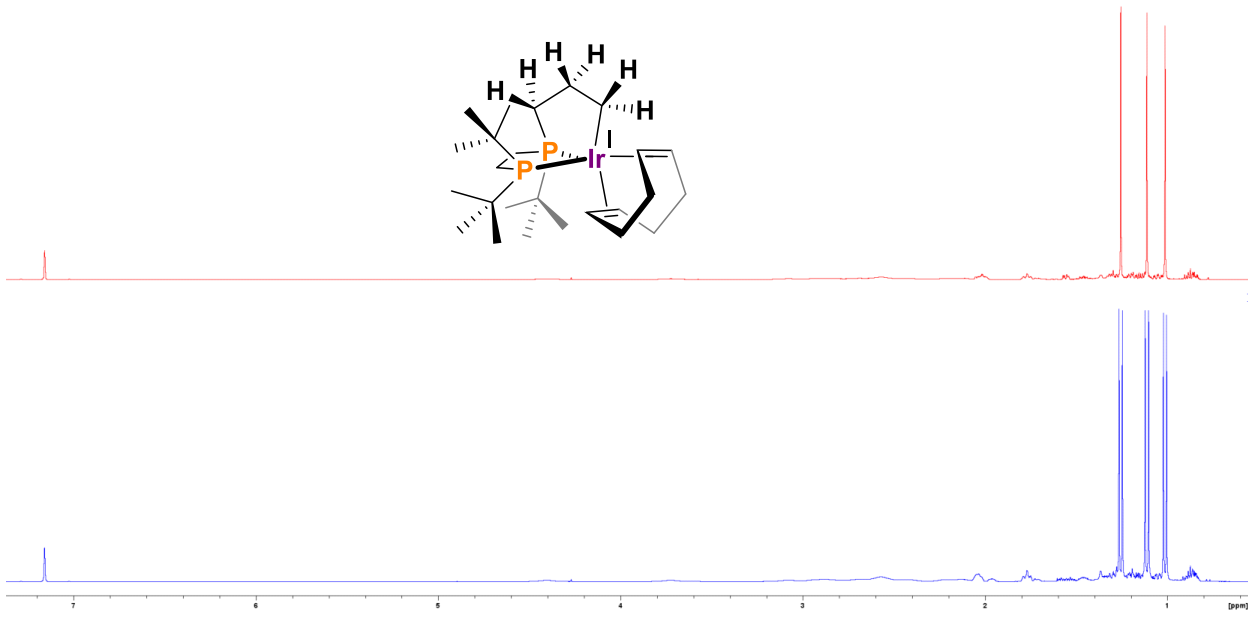

Figure S5. (±)-1, $^{31}P\{^{1}H\}$ NMR, C_6D_6, 121 MHz, 298 K.

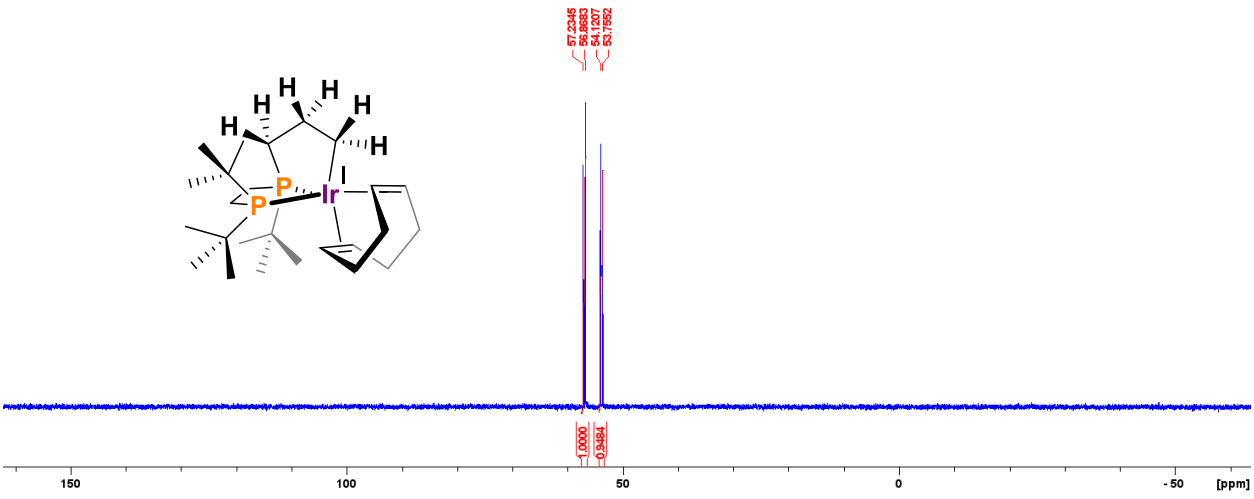

Figure S6. (±)-1, $^{13}C\{^{1}H\}$ NMR, C_6D_6, 151 MHz, 298 K.

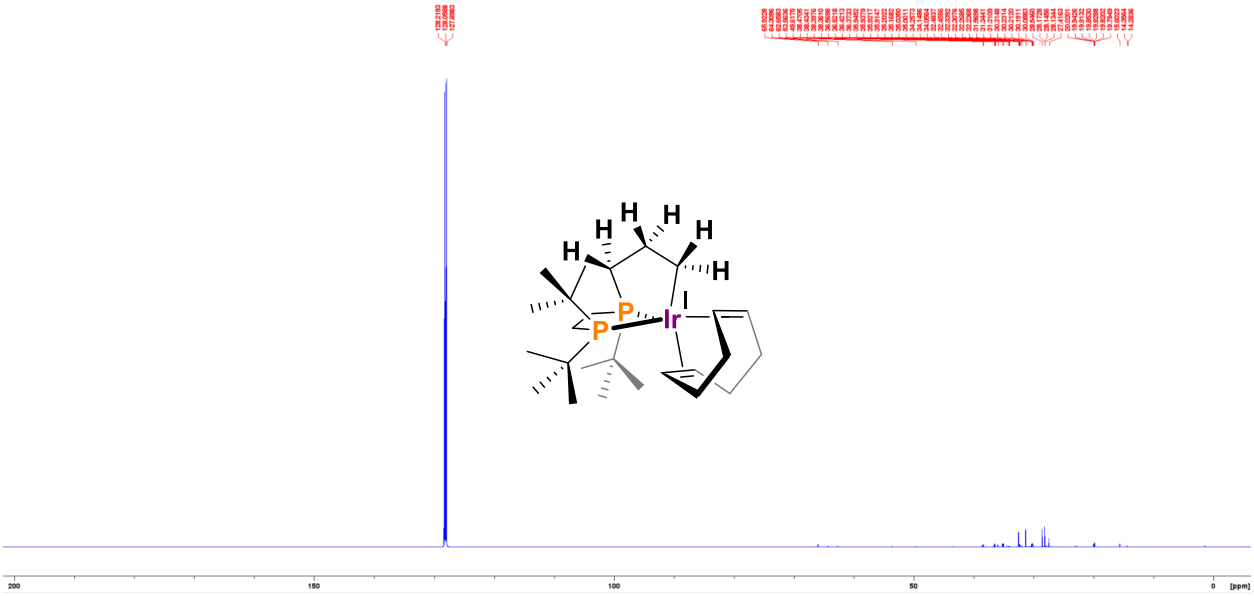

Figure S7. (±)-1, $^{13}C\{^{1}H\}$ NMR (expansion), C_6D_6, 151 MHz, 298 K.

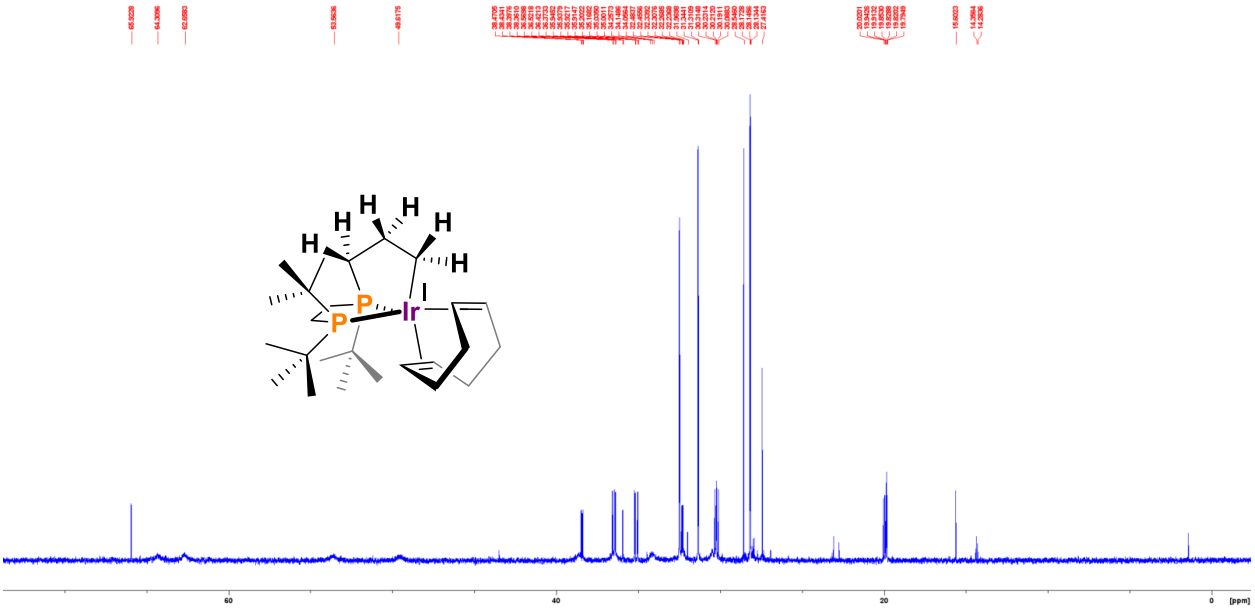

Figure S8. (±)-2, ^{1}H NMR, C_6D_6, 600 MHz, 298 K.

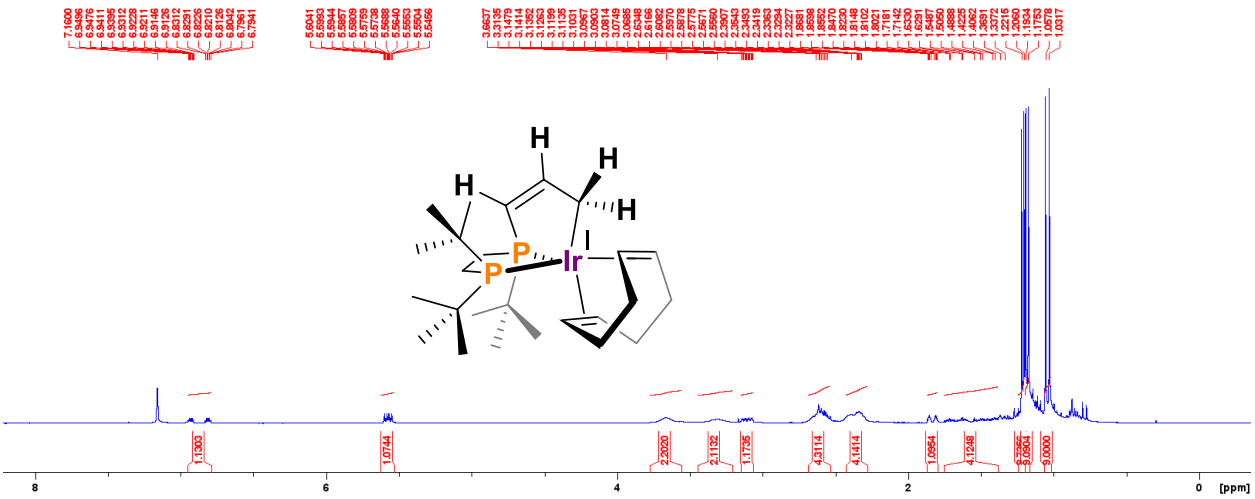

Figure S9. (±)-2, ^{1}H NMR (expansion), C_6D_6, 600 MHz, 298 K.

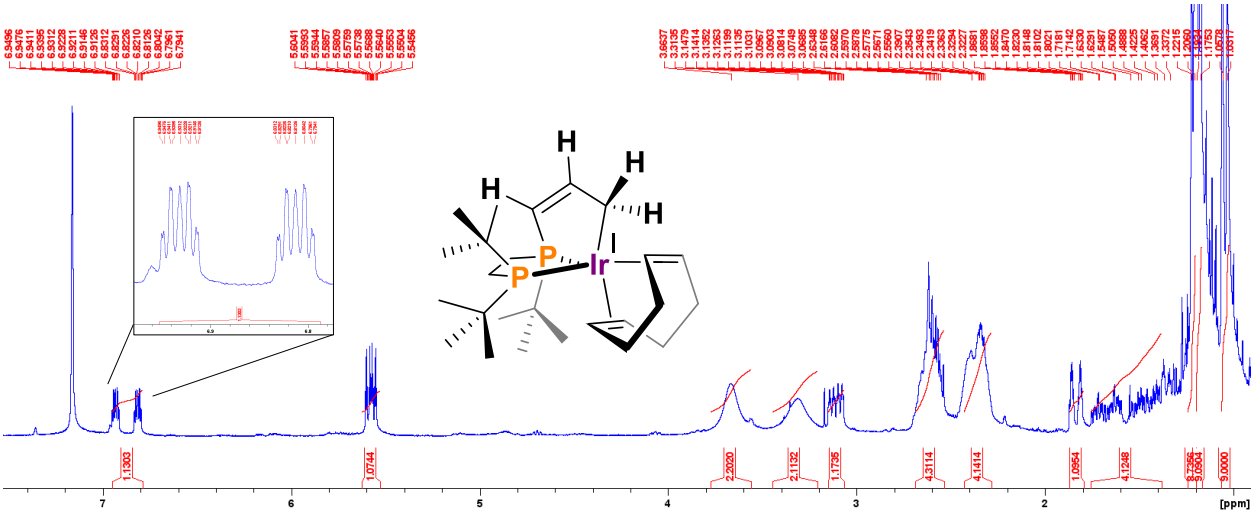

Figure S10. (±)-2, $^{1}H\{^{31}P\}$ NMR, C_6D_6, 600 MHz, 298 K.

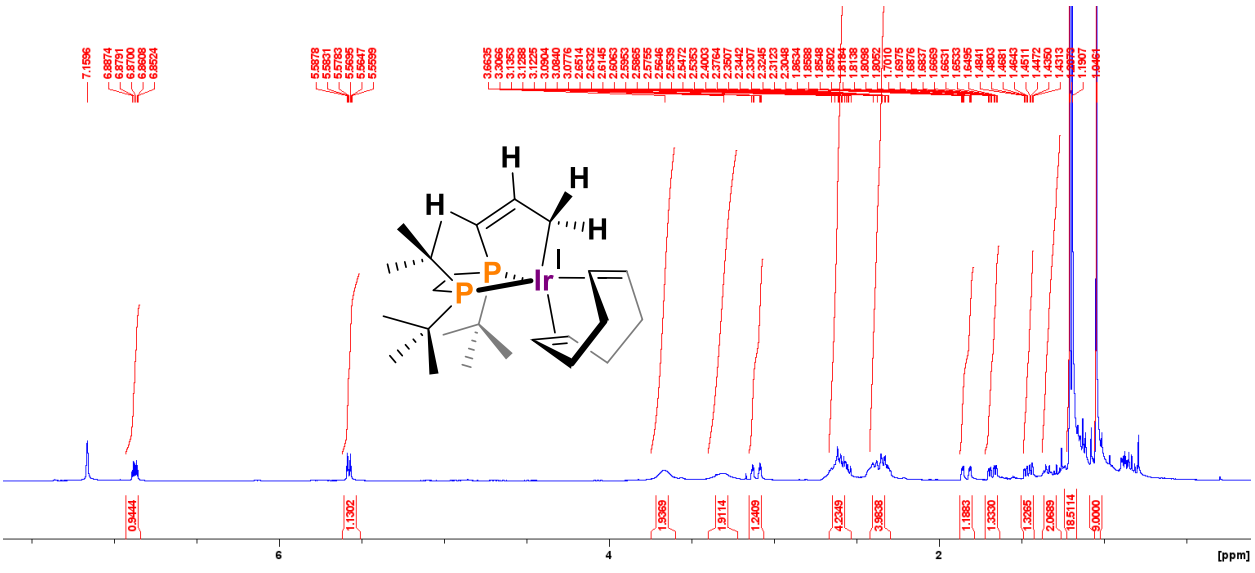

Figure S11. (±)-2, ^{1}H (blue)/$^{1}H\{^{31}P\}$ (red) NMR, C_6D_6, 600 MHz, 298 K.

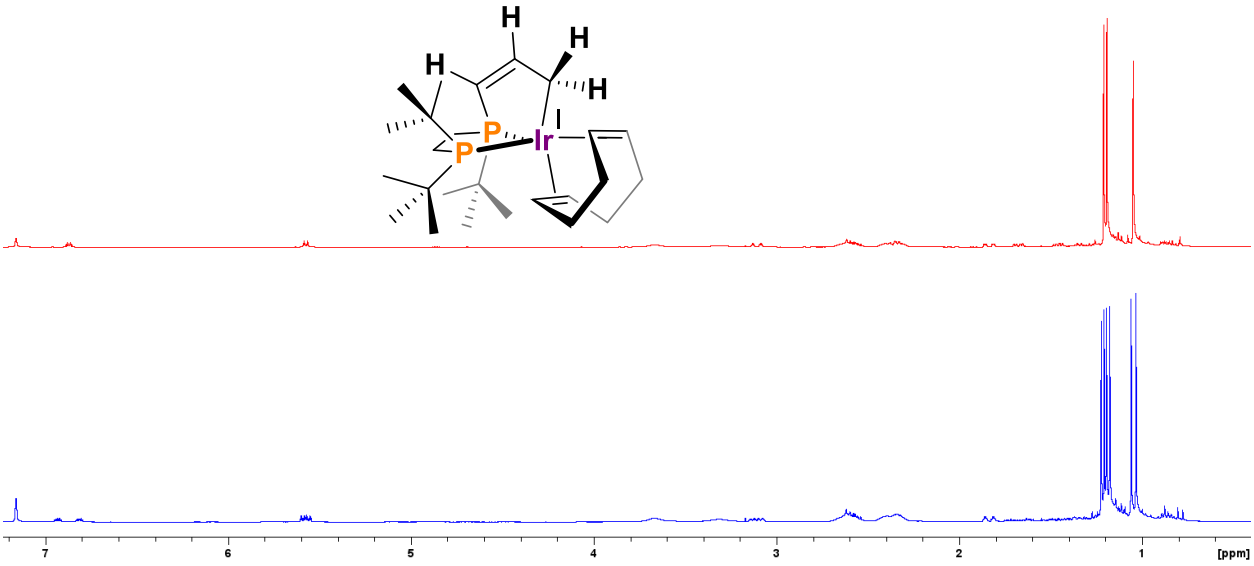

Figure S12. (±)-2, ^{1}H (blue)/$^{1}H\{^{31}P\}$ (red) NMR (expansion), C_6D_6, 600 MHz, 298 K.

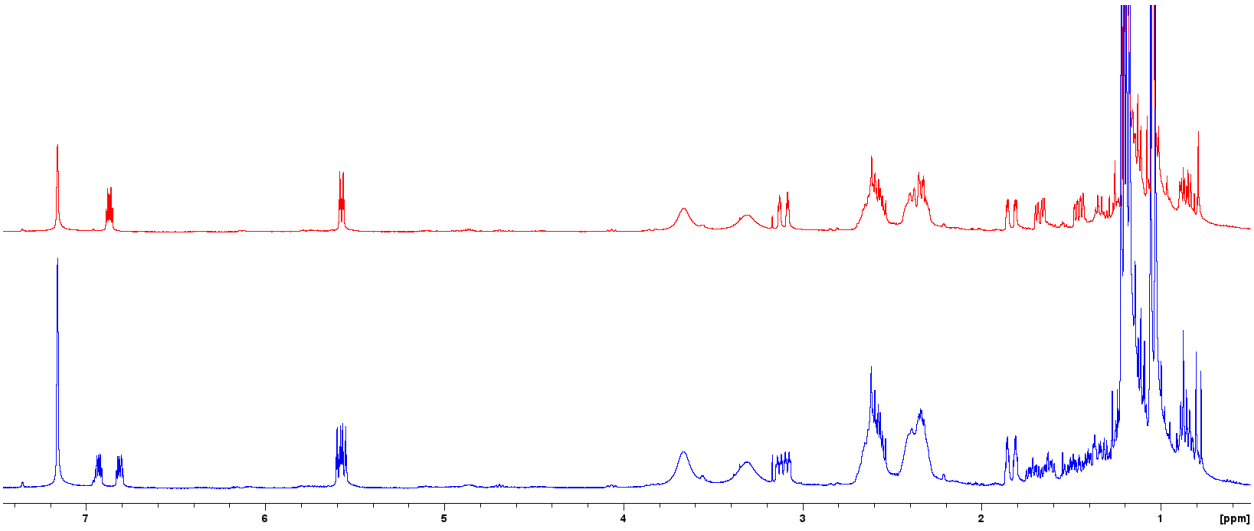

Figure S13. (±)-2, $^{31}P\{^{1}H\}$ NMR, C_6D_6, 121 MHz, 298 K, [**(±)-3** δ_P = 69.0/34.4].

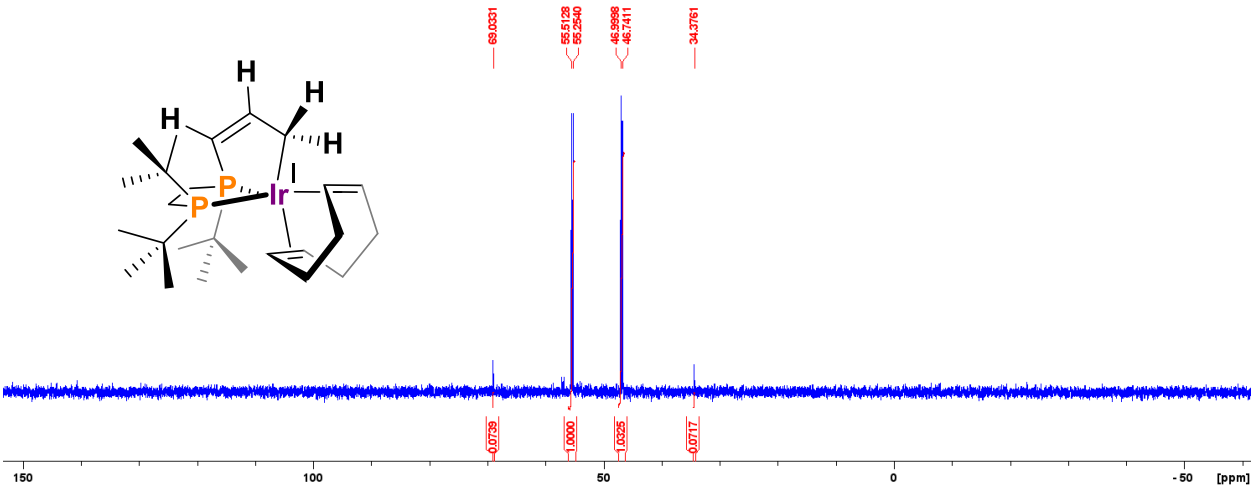

Figure S14. (±)-2, $^{13}C\{^{1}H\}$ NMR, C_6D_6, 151 MHz, 298 K.

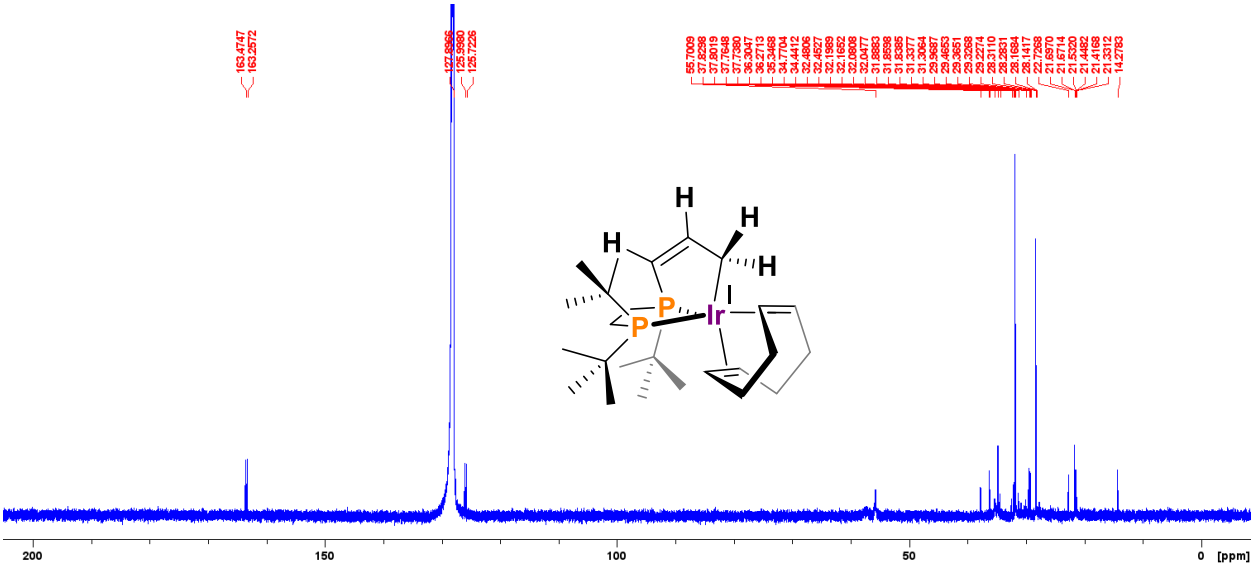

Figure S15. (±)-2, ^{1}H-^{1}H COSY NMR, C_6D_6, 600 MHz, 298 K.

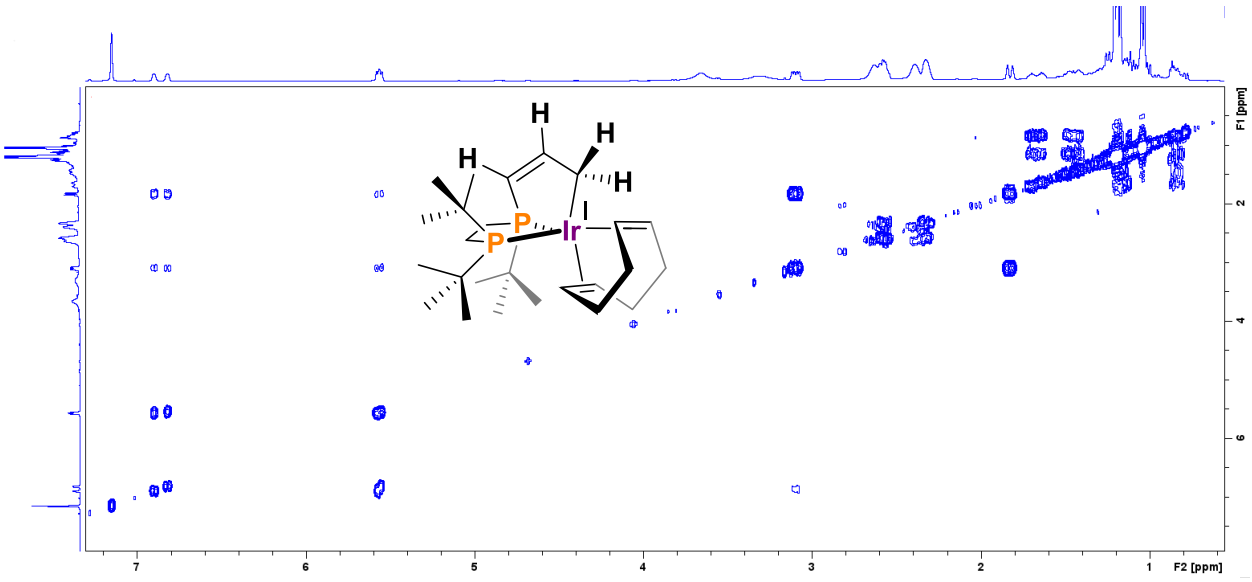

Figure S16. (±)-3, ^{1}H NMR, C_6D_6, 600 MHz, 298 K.

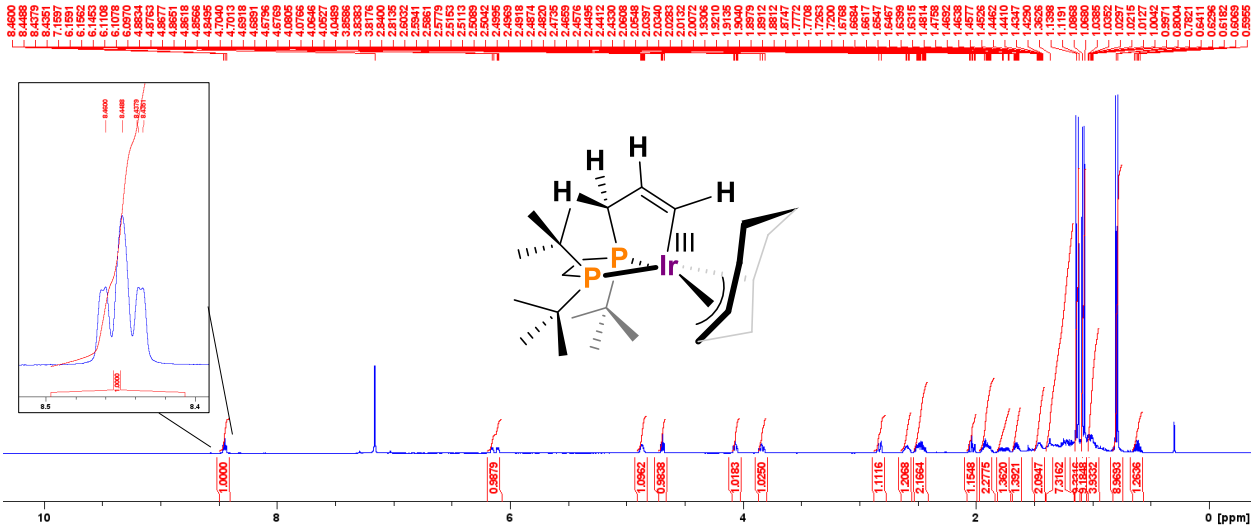

Figure S17. (±)-3, ^{1}H NMR (expansion), C_6D_6, 600 MHz, 298 K.

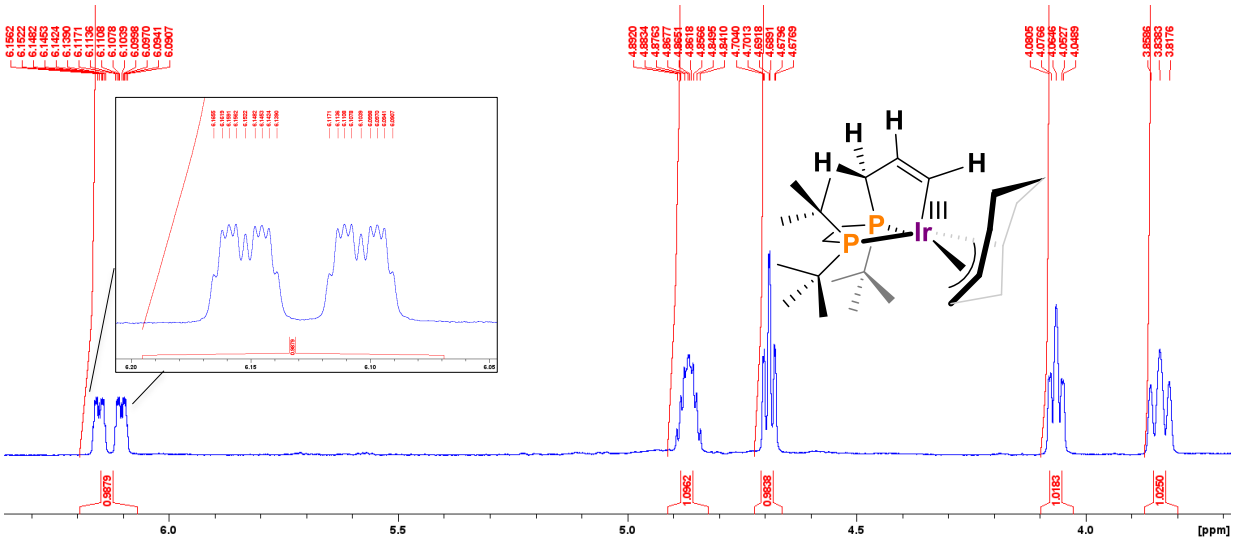

Figure S18. (±)-3, ^{1}H NMR (expansion), C_6D_6, 600 MHz, 298 K.

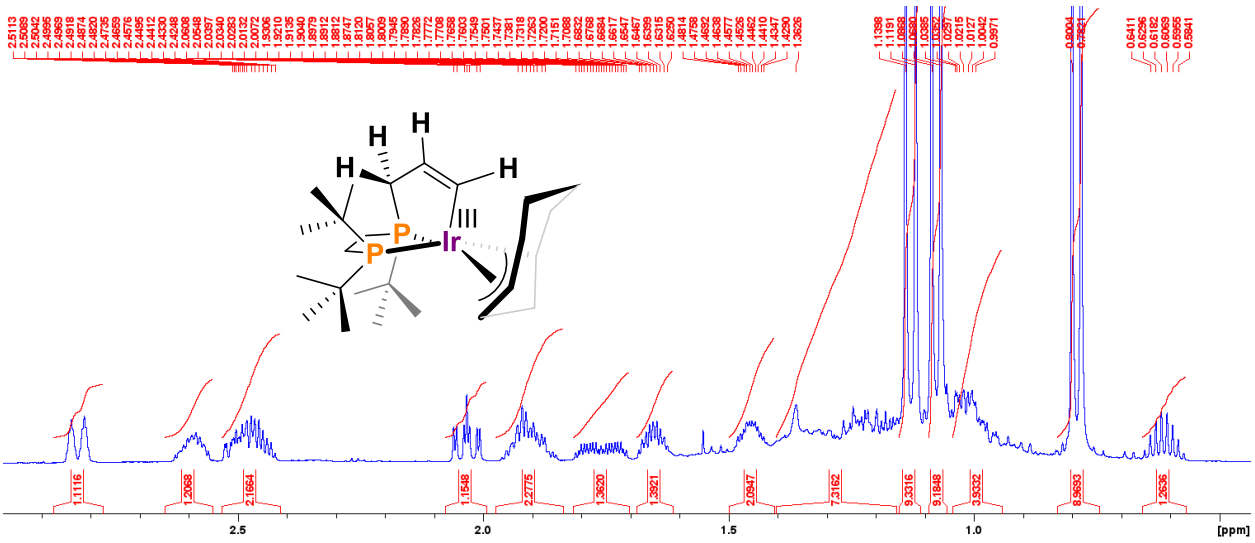

Figure S19. (±)-3, $^{1}H\{^{31}P\}$ NMR, C_6D_6, 600 MHz, 298 K.

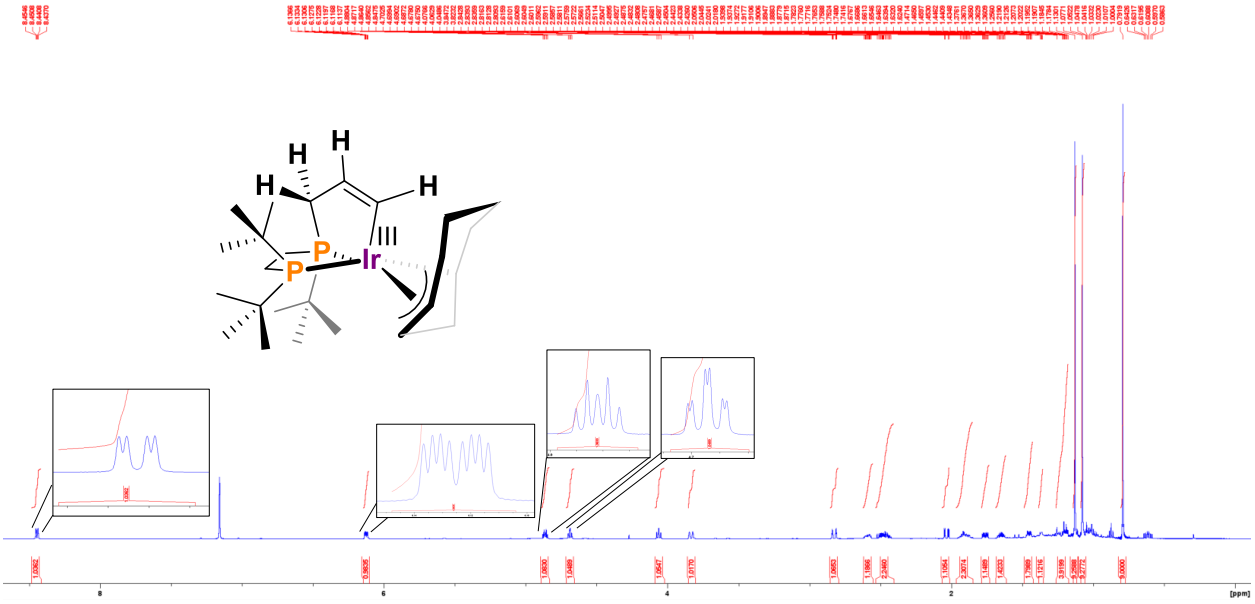

Figure S20. (±)-3, ^{1}H (blue)/ $^{1}H\{^{31}P\}$ (red) NMR Stacked, C_6D_6, 600 MHz, 298 K.

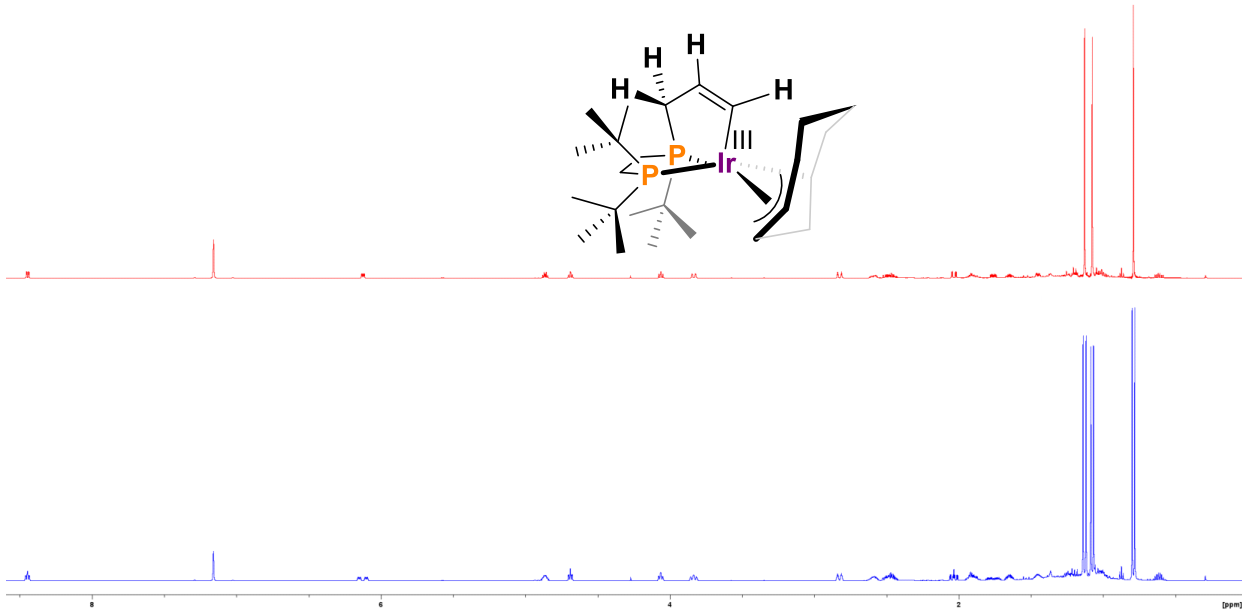

Figure S21. (±)-3, ^{1}H (**blue**)/$^{1}H\{^{31}P\}$ (**red**) NMR Stacked (expansion), C_6D_6, 600 MHz, 298 K.

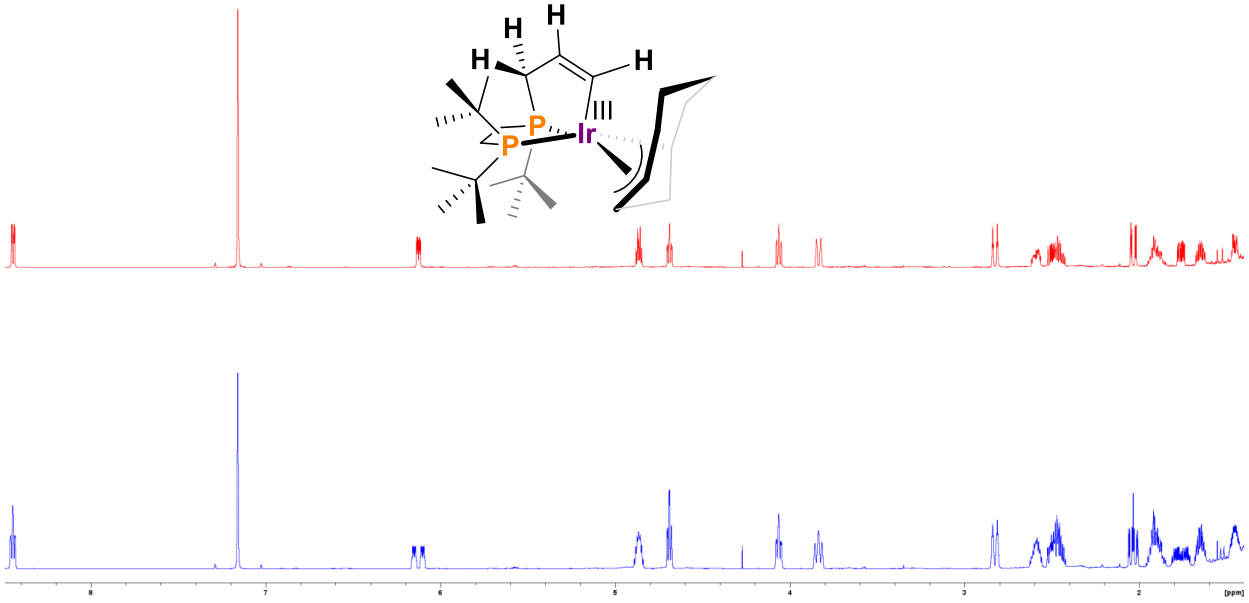

Figure S22. (±)-3, $^{31}P\{^{1}H\}$ NMR, C_6D_6, 243 MHz, 298 K.

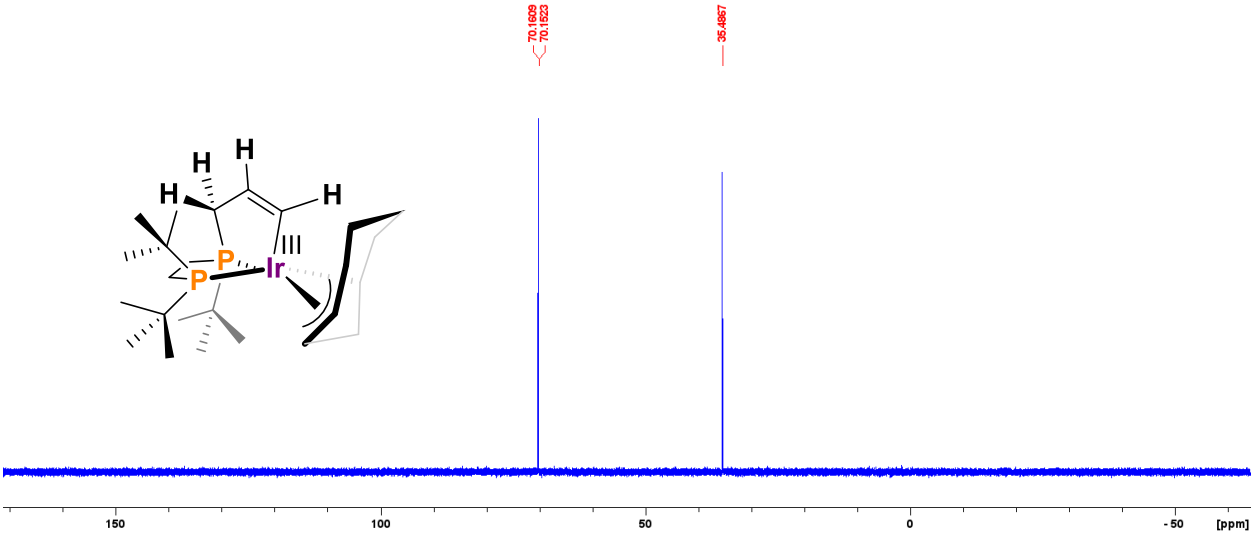

Figure S23. (±)-3, $^{13}C\{^{1}H\}$ NMR, C_6D_6, 151 MHz, 298 K.

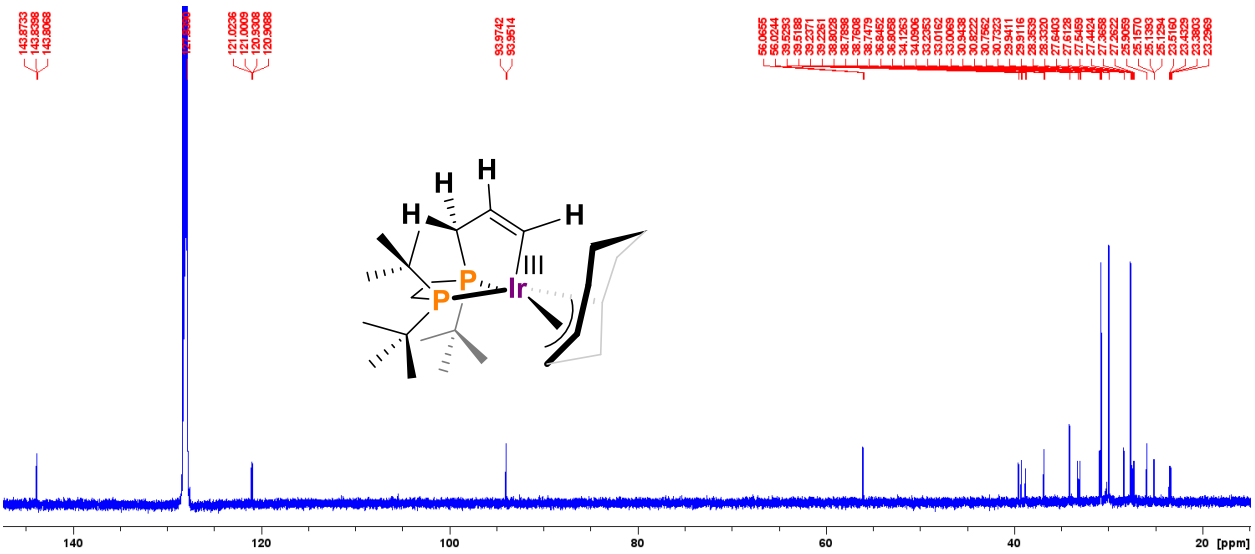

Figure S24. (±)-3, ^{1}H-^{1}H COSY NMR, C_6D_6, 600 MHz, 298 K.

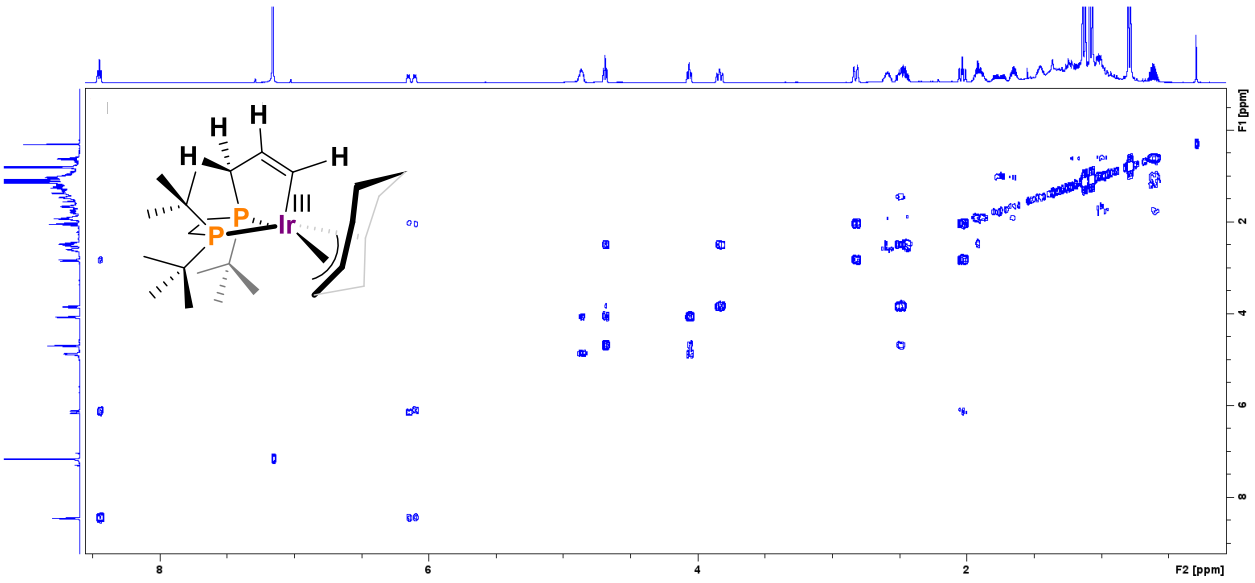

Figure S25. (±)-3, ^{1}H-$^{13}C\{^{1}H\}$ HSQC NMR, C_6D_6, 600 MHz, 298 K.

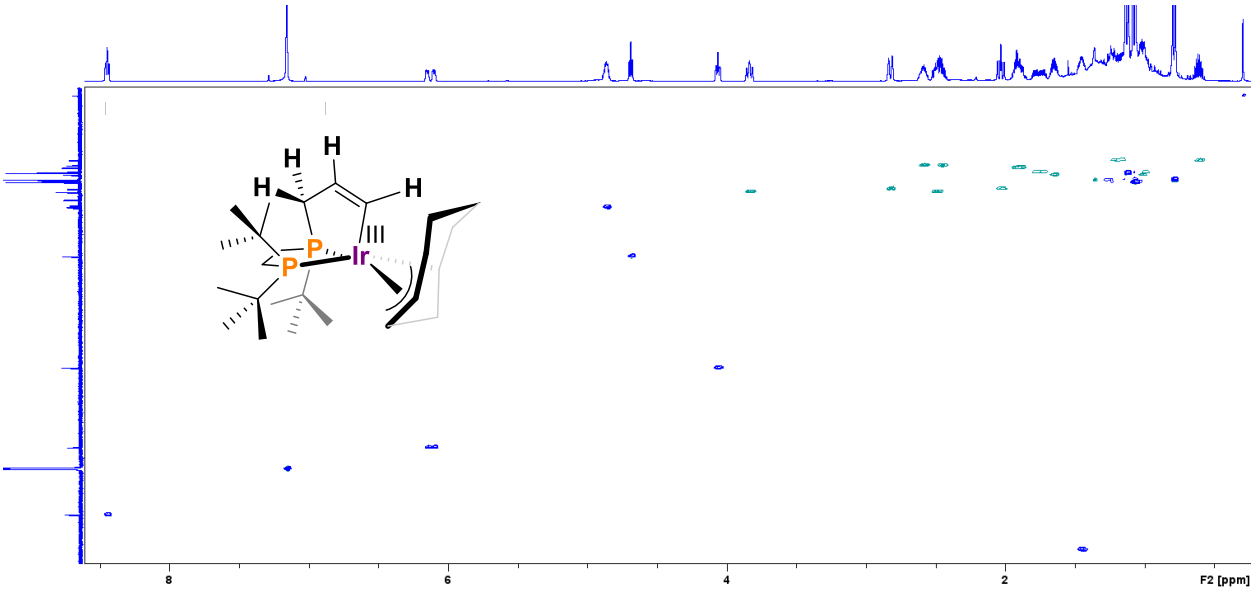

Figure S26. t^{t}bape-d$_5$, $^{31}P\{^{1}H\}$ NMR, C_6D_6, 243 MHz, 298 K (Impurity at δ_P = -5.64 & 34.8 is $(^{t}Bu)_2PCH_2CH_2P(^{t}Bu)$-$P(^{t}Bu)CH_2CH_2P(^{t}Bu)_2$).

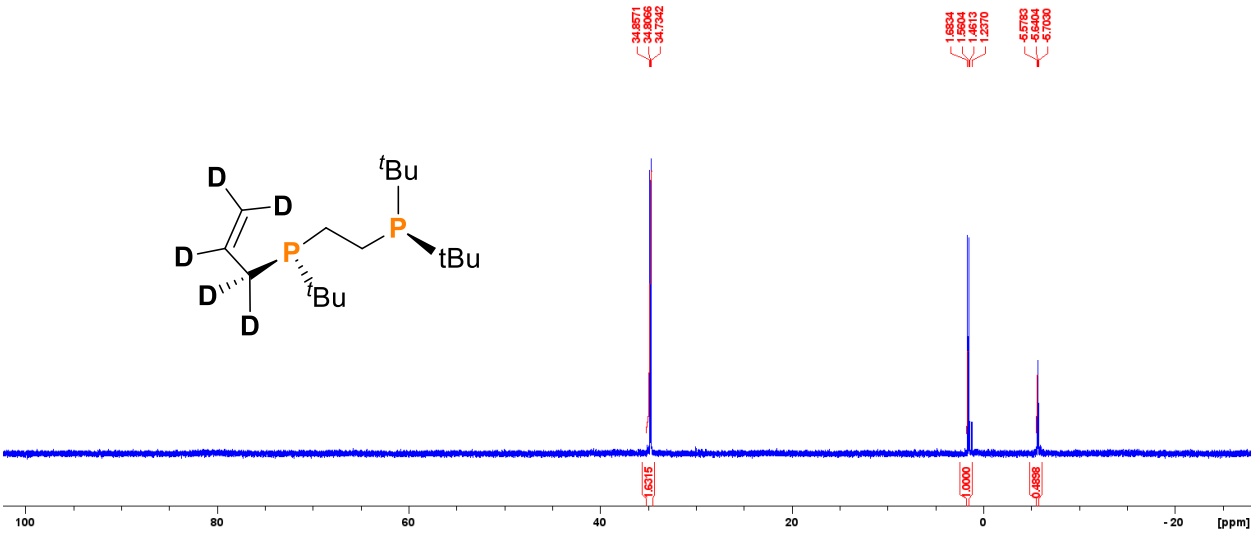

Figure S27. t^{t}bape-d$_5$, ^{1}H NMR, C_6D_6, 600 MHz, 298 K.

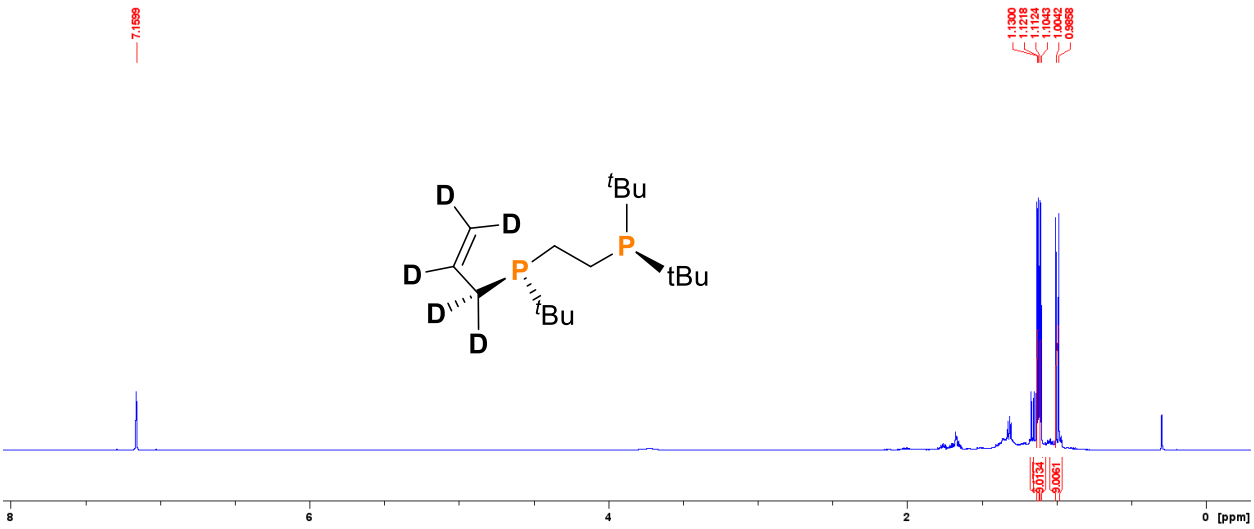

Figure S28. t^{t}bape-d$_5$ (blue) and **t^{t}bape** (red) overlay, ^{31}P{^{1}H} NMR, C_6D_6, 243 MHz, 298 K.

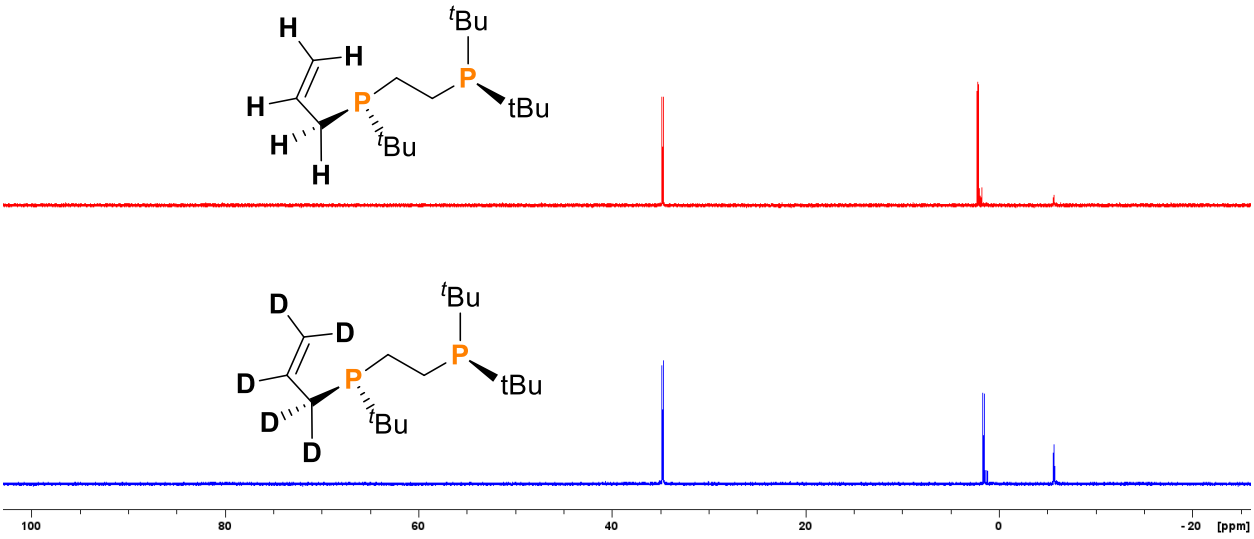

Figure S29. t^{t}bape-d$_5$ (blue) and **t^{t}bape** (red), ^{1}H NMR, C_6D_6, 600 MHz, 298 K.

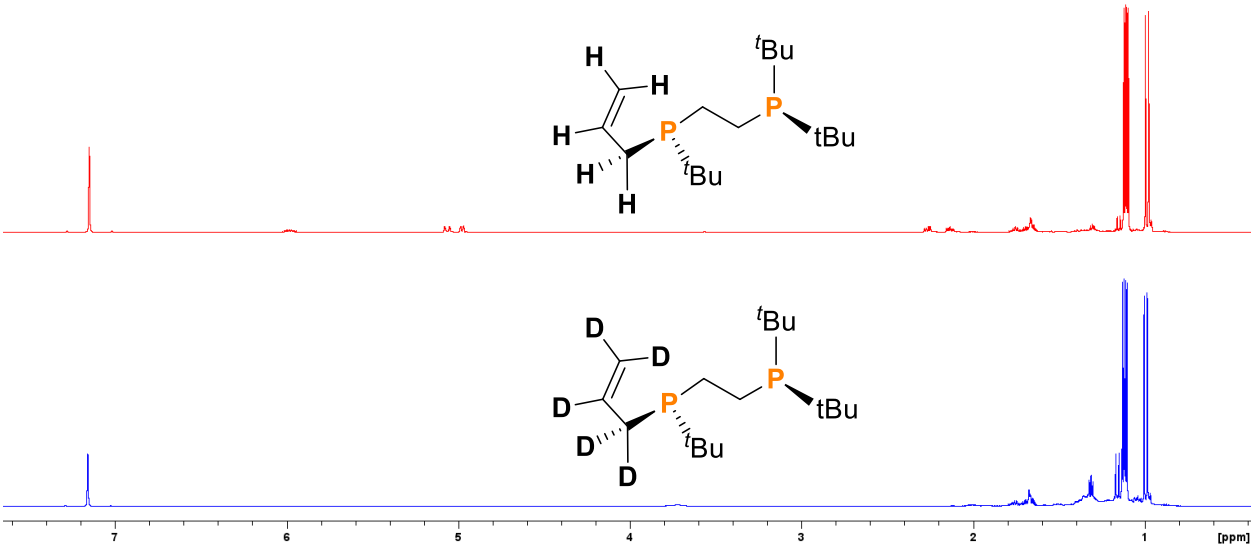

Figure S30. t^{t}bape-d$_5$ (blue) and **t^{t}bape** (red) (expansion), ^{1}H NMR, C_6D_6, 600 MHz, 298 K.

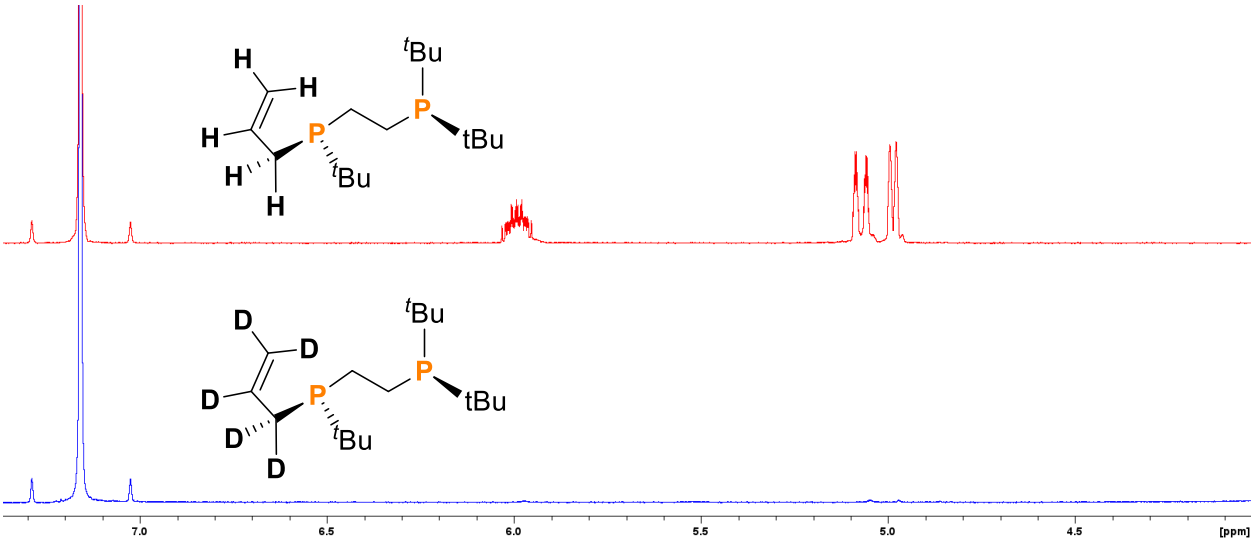

Figure S31. (±)-3-d4, ^{1}H NMR, C_6D_6, 600 MHz, 298 K.

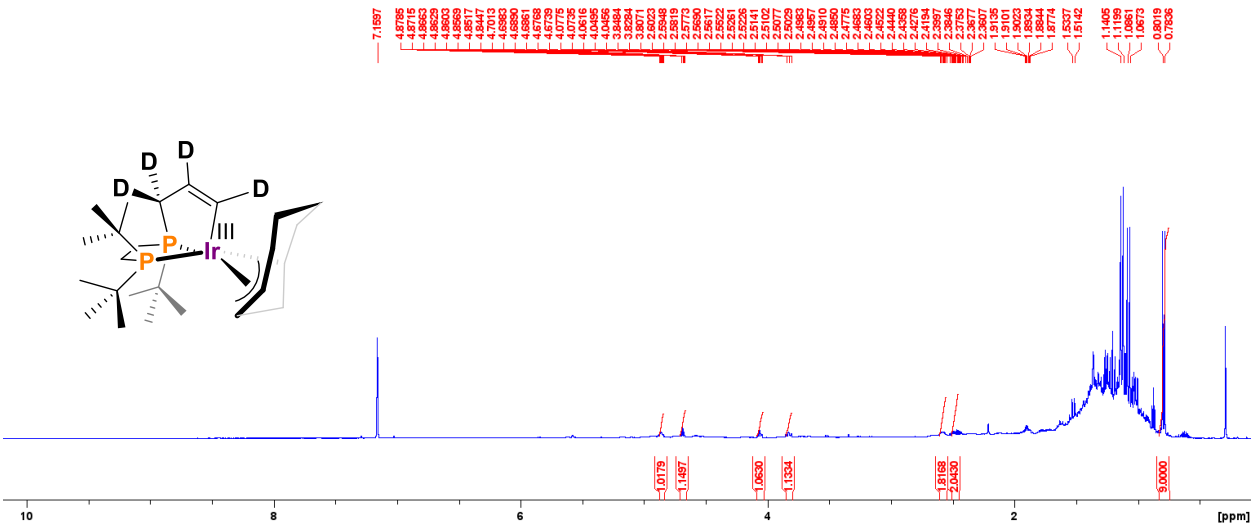

Figure S32. (±)-3-d4, $^{31}P\{^{1}H\}$ NMR, C_6D_6, 243 MHz, 298 K.

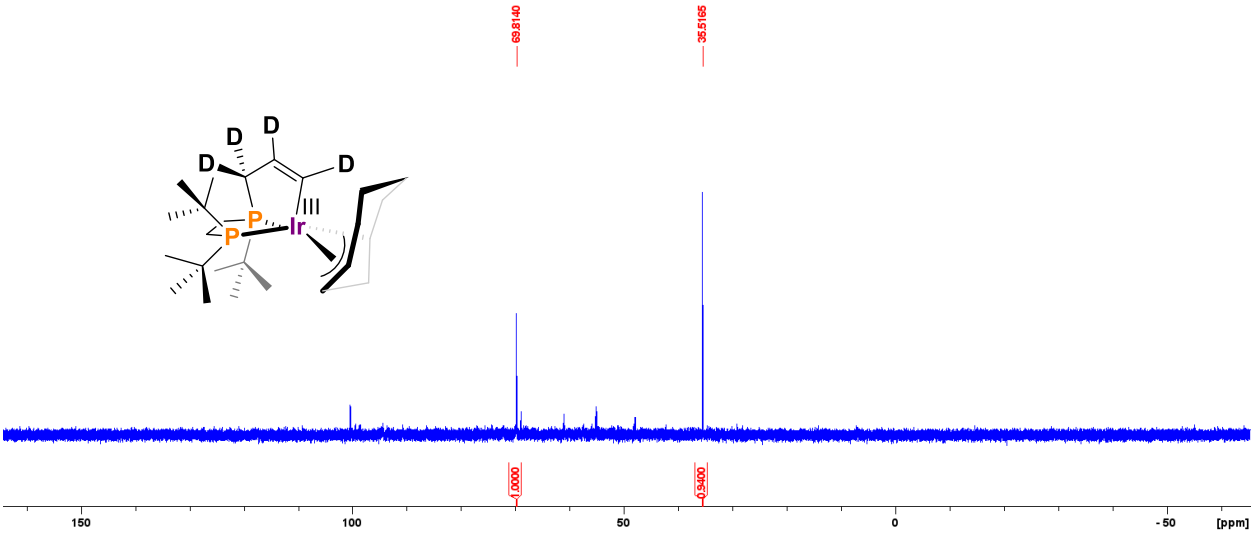

Figure S33. (±)-3-d$_4$ (blue) and **(±)-3** (red) overlay, $^{31}P\{^1H\}$ NMR, C_6D_6, 243 MHz, 298 K.

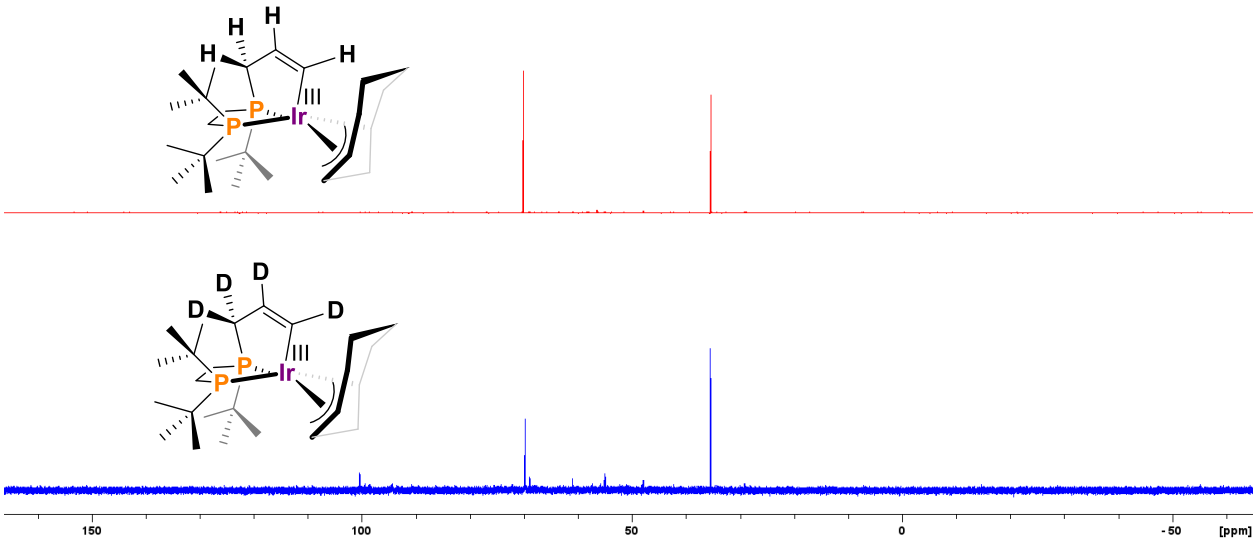

Figure S34. (±)-3-d$_4$ (blue) and **(±)-3** (red) overlay, ^1H NMR, C_6D_6, 600 MHz, 298 K. (Signals at δ_H = 8.45, 6.13, 2.83, and 2.04 ppm are absent).

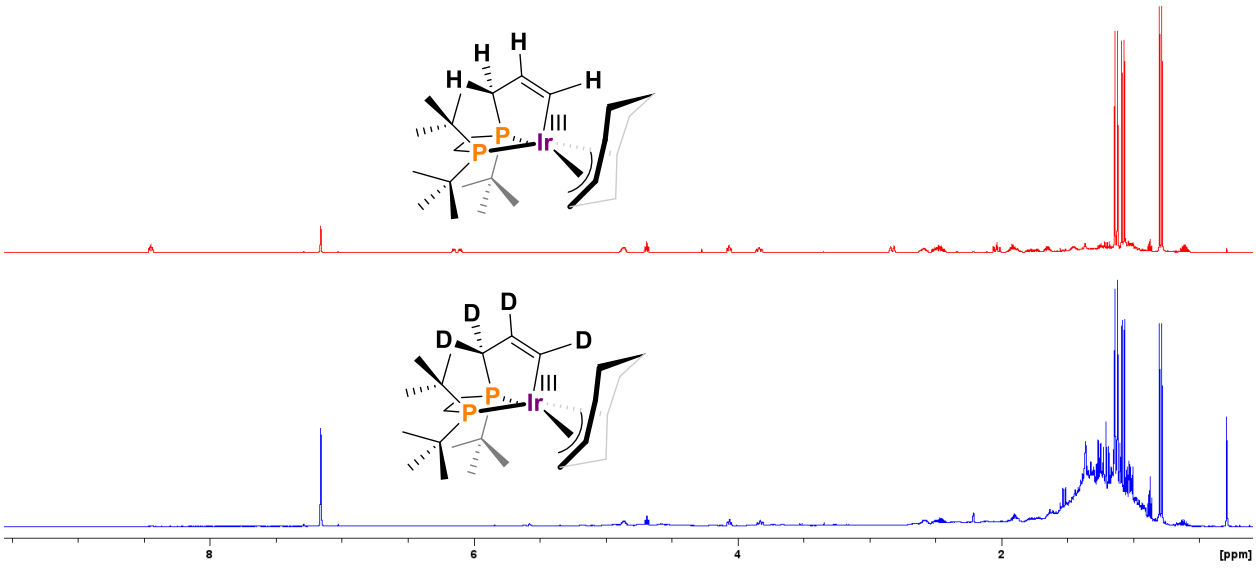

Figure S35. (±)-3-d$_4$ (blue) and **(±)-3** (red) overlay, ^{1}H NMR, C_6D_6, 600 MHz, 298 K. (Signals at δ_H = 8.45, 6.13, 2.83, and 2.04 ppm are absent – highlighted below).

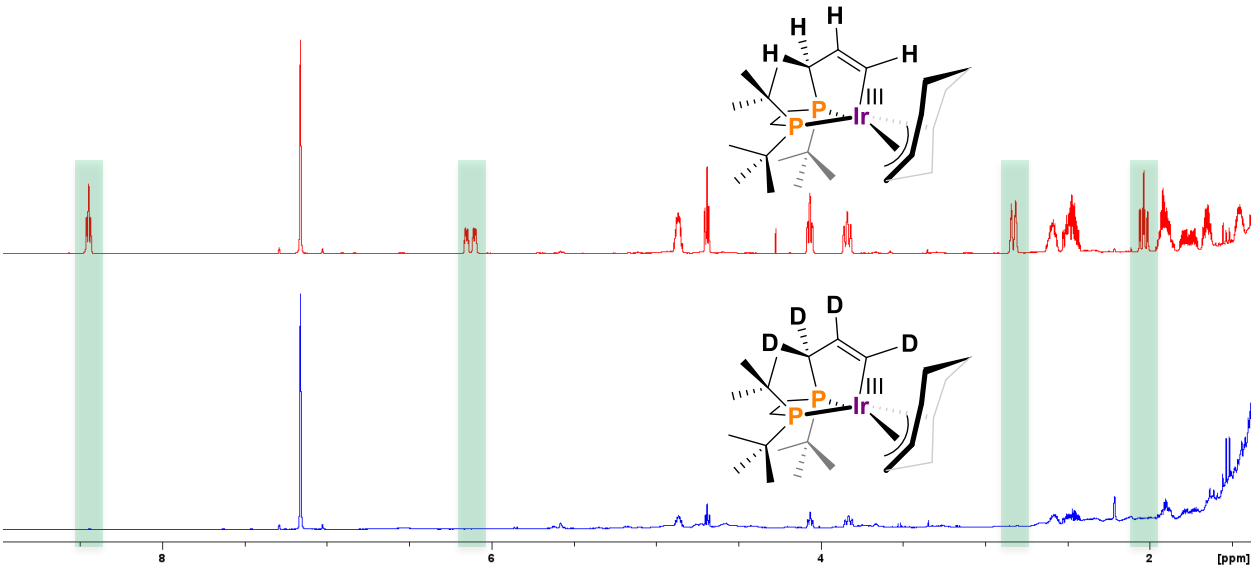

IR Data

Figure S36. (±)-1, FT-IR (ATR), thin film from evaporated C_6D_6.

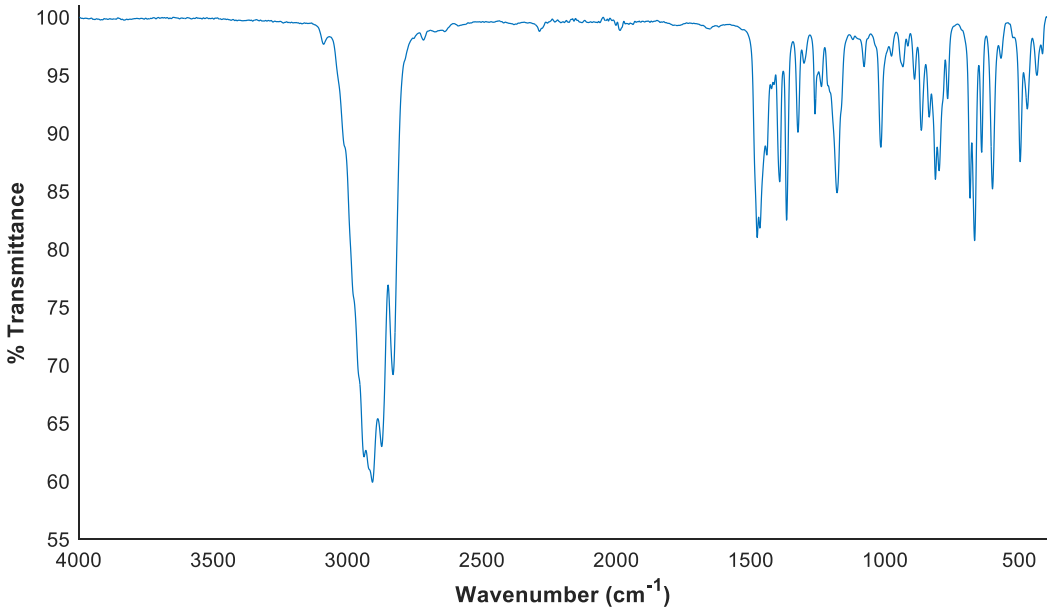

Figure S37. (±)-2, FT-IR (ATR), thin film from evaporated C_6D_6.

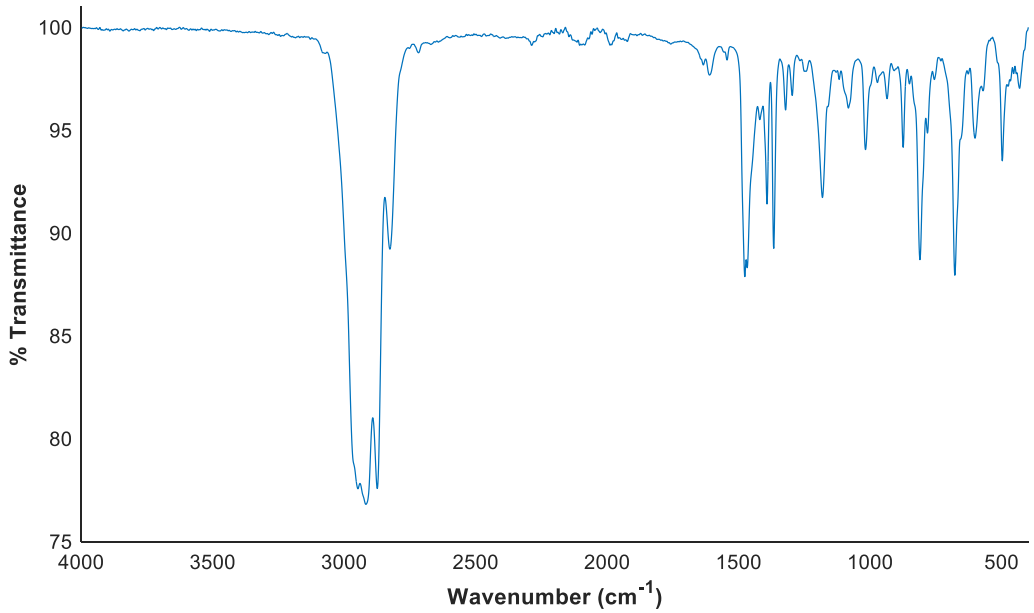

Figure S38. (±)-3, FT-IR (ATR), thin film from evaporated C_6D_6.

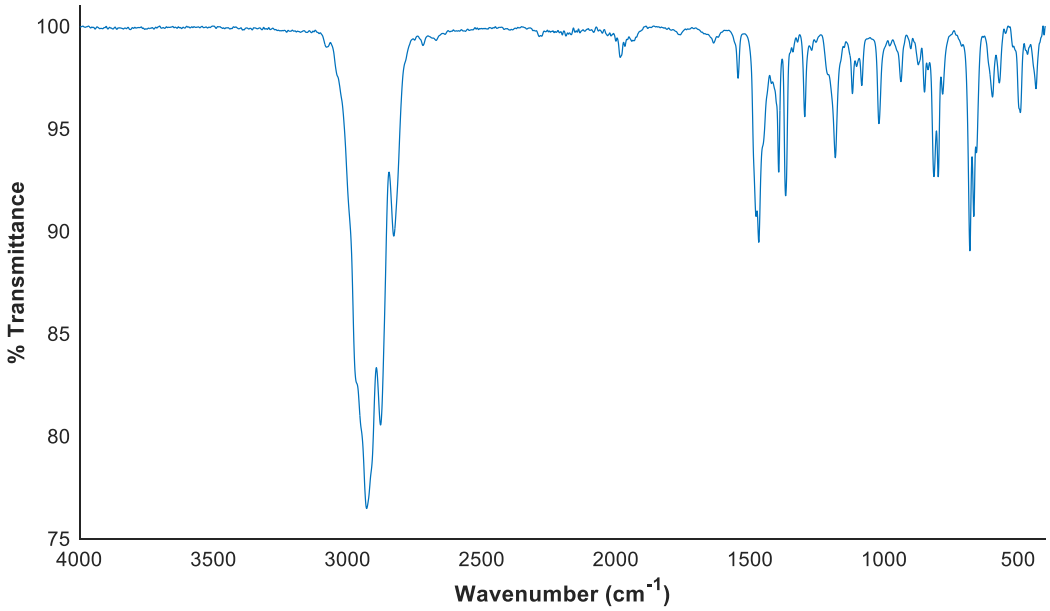

Figure S39. [Ir(μ-OMe)COD]$_2$, FT-IR (ATR), thin film from evaporated C_6D_6

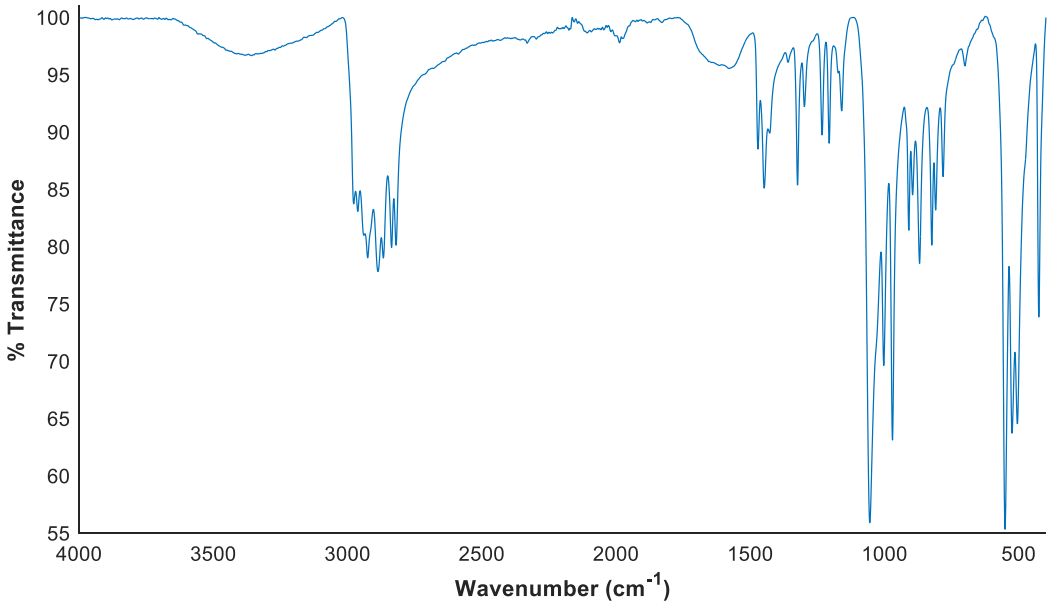

Figure S40. t^tbape, FT-IR (ATR), thin film from evaporated C_6D_6.

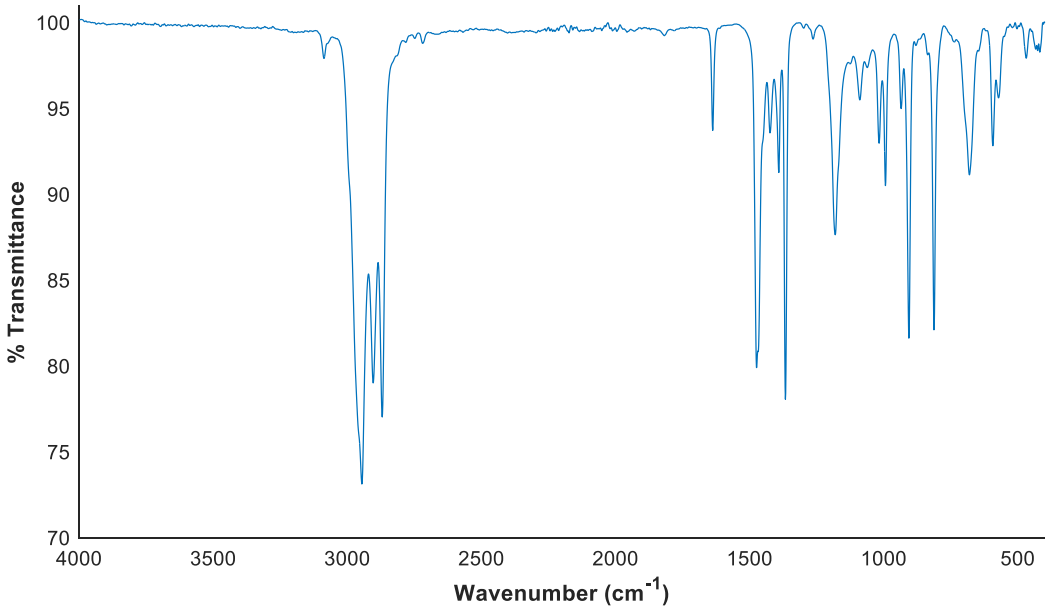

Figure S41. t^tbbpe, FT-IR (ATR), thin film from evaporated C_6D_6.

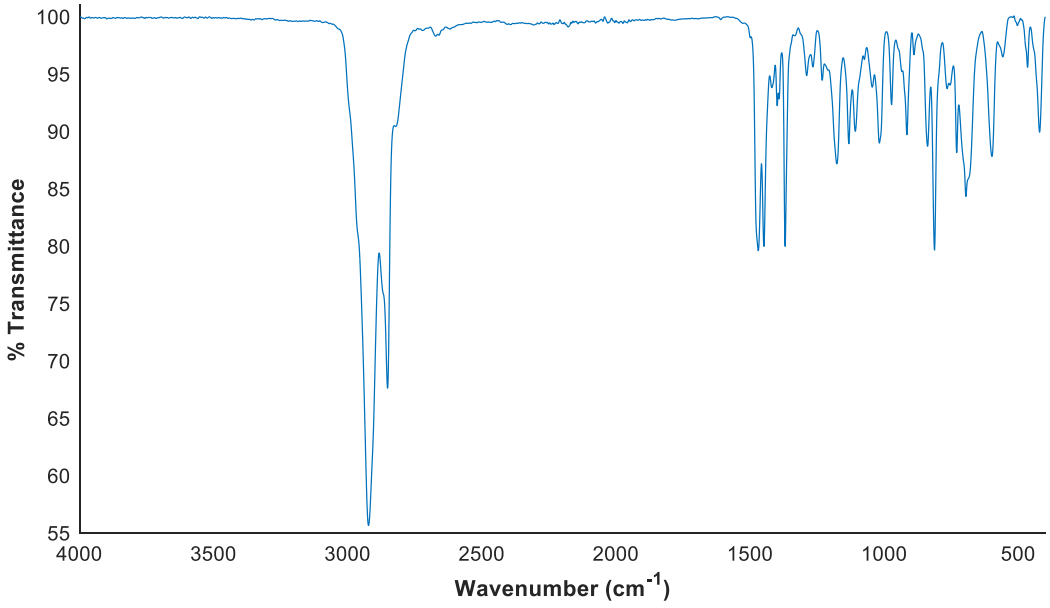

Computational details

All calculations were performed using version 5.0.3 of the ORCA computational package.[3] All geometry optimizations and frequency calculations were performed at the PBE0-D3(BJ)/def2-TZVP level of theory.[4] The SARC-ZORA-TZVP basis set was used for iridium (along with the *SARC/J* auxiliary basis). The RIJCOSX approximation was used to enhance computational efficiency, along with the auxiliary basis *def2/J*.[5] Convergence criteria were met using the *defgrid2* integral grid size. Frequency calculations (*Freq*) were performed to confirm that each optimized geometry was a true minimum indicated by the absence of imaginary frequencies. A Universal Solvation Model (SMD) of benzene was used to calculate the thermodynamic parameters.

Accurate electronic energies were determined using CCSD(T) at the DLPNO-CCSD(T)/def2-TZVP level of theory.[6] The RIJCOSX approximation was used to enhance computational efficiency, along with a *def2/*J auxiliary basis set.[7] As well, a *def2-TZVP/C* auxiliary basis set was used.[8]

To obtain accurate thermochemical information, the final Gibbs free energies for each chemical species were calculated using the following equation.

$$\Delta G_{solv} = E_{el}(DLPNO\text{-}CCSD(T)) + \Delta G_{correction}(DFT) + \Delta G^{\circ}_{solv}(DFT)$$

$E_{el}(DLPNO\text{-}CCSD(T))$ is the final electronic energy from a DLPNO-CCSD(T)/def2-TZVP calculation, $\Delta G_{correction}(DFT)$ is the $G\text{-}E_{el}$ (Gibbs free energy minus the electronic energy) from a BP86-D3(BJ)/def2-TZVP calculation, and $\Delta G^{\circ}_{solv}(DFT)$ is the sum of $\Delta G_{ENP}(CPCM\ Dielectric)$ and $\Delta G_{CDS}(Free\text{-}energy(cav+disp))$ from an *SMD* single point calculation.

Geometries of optimized molecules can be retrieved from a .xyz file associated with this work.

Discussion of conversion of IV to (±)-3:

To probe thermodynamics for the conversion of **IV** to **(±)-3**, relative energies were compared, providing G_{rel} = 1.7 kcal mol^{-1} on going from the 1,2,3,6-η^3,η^1-C_8H_{12} (**IV**) to 1,2,3,5-η^3,η^1-C_8H_{12} (**(±)-3**) binding motif. On inspection, however, it would appear that the 1,2,3,5-η^3,η^1-C_8H_{12} isomer does contain the less distorted octahedron (taking C1, C5, and the two phosphines as the equatorial plane).

Figure S41. Energetic comparison between **IV** and **(±)-3**.

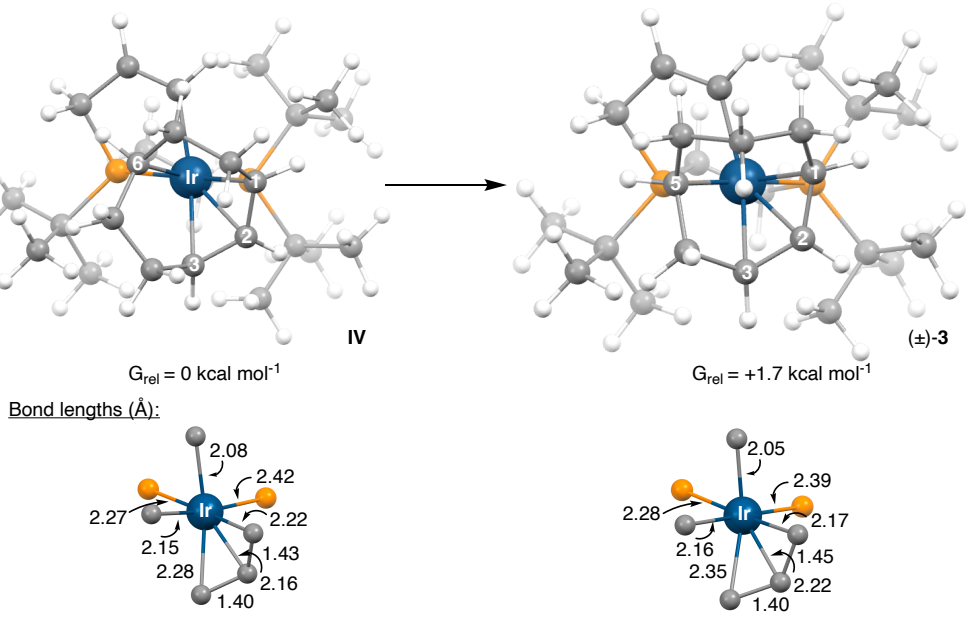

Crystallographic details:

Single crystal X-ray diffraction (scXRD) data for **(±)-1** and **(±)-2** was collected using a Bruker D8 Venture diffractometer equipped with an Apex detector and IμS Cu microsource at the University of Windsor. Both crystals were mounted on a MiTeGen loop. Data for **(±)-1** and **(±)-2** was obtained using Molybdenum K-α, $\lambda = 0.71$ Å at 170(2) K. Cell refinement and data reduction were performed using Apex3. [9] An empirical absorption correction, based on the multiple measurements of equivalent reflections and merging of data was performed using SADABS.[10] Data conversion from XDS to SADABS file format was performed using XDS2SAD.[11] The space group was confirmed by XPREP.[12]

Single crystal X-ray diffraction (scXRD) data for **(±)-3** was obtained using a Mitegen polyimide micromount with a small amount of Paratone N oil. All X-ray measurements were made on a Bruker Kappa Axis Apex2 diffractometer at Western University. The unit cell dimensions were determined from a symmetry constrained fit of 9760 reflections with $4.84° < 2\theta < 60.92°$. The data collection strategy used φ and ω scans which collected data up to 61.06° (2θ). The frame integration was performed using SAINT.[13] The resulting raw data was scaled, and absorption corrected using a multi-scan averaging of symmetry equivalent data using SADABS.[14]

Routine checkCIF and structure factor analyses were performed using Platon.[15] CCDC **2311411-2311413** contains the supplementary crystallographic data for this paper. These data can be obtained free of charge from The Cambridge Crystallographic Data Centre *via* www.ccdc.cam.ac.uk/data_request/cif.

Table S2. Crystallographic data for **(±)-1** and **(±)-2**.

Compound	**(±)-1**	**(±)-2**
Empirical formula	$C_{25}H_{49}IrP_2$	$C_{25}H_{47}IrP_2$
Formula weight	603.78	601.76
Temperature/K	170.0	170.0
Crystal system	Orthorhombic	Orthorhombic
Space group	*Pbca*	*Pbca*
a/Å	17.8681(5)	10.0014(3)
b/Å	14.8775(4)	17.1653(5)
c/Å	38.0030(10)	28.5541(9)
α/°	90	90
β/°	90	90
γ/°	90	90
V/Å^3	10102.4(5)	4901.6(3)
Z	16	8
ρ_{calc} g/cm^{-3}	1.588	1.631
μ/ mm^{-1}	5.423	5.588
F(000)	4896.0	2432.0
Crystal size/ mm^3	0.12 × 0.11 × 0.08	0.15 × 0.1 × 0.07
Radiation	MoKα (λ = 0.71073)	MoKα (λ = 0.71073)
2θ range for datacollection/°	3.72 to 56.672	4.746 to 56.632
Index ranges	-23 ≤ h ≤ 23, -19 ≤ k ≤ 19, -50 ≤ l ≤ 60	-13 ≤ h ≤ 13, -22 ≤ k ≤ 22, -38 ≤ l ≤ 37
Independent reflections	12555 [R_{int} = 0.0940, R_{sigma} = 0.0209]	6082 [R_{int} = 0.0441, R_{sigma} = 0.0177]
Data/restraints/parameters	12555/27/507	6082/0/263
Goodness-of-fit on F^2	1.207	1.149
R [I>=2θ (I)] (R1, wR2)	R_1 = 0.0540, wR_2 = 0.1090	R_1 = 0.0204, wR_2 = 0.0445
R (all data) (R1, wR2)	R_1 = 0.0716, wR_2 = 0.1191	R_1 = 0.0238, wR_2 = 0.0465
Largest diff. peak/hole / (e Å^{-3})	6.37/-3.69	1.90/-1.10

$R1 = \Sigma \, ||F_o|-|F_c|| \, / \, \Sigma \, |F_o|$; $wR2 = [\Sigma(w(F_o^2 - F_c^2)^2) \, / \, \Sigma \, w(F_o^2)^2]^{1/2}$

Table S3. Crystallographic data for **(±)-3**.

Compound	**(±)-3**
Empirical formula	$C_{25}H_{47}IrP_2$
Formula weight	601.76
Temperature/K	110.0
Crystal system	Monoclinic
Space group	$P2_1/c$
a/Å	10.405(9)
b/Å	18.494(13)
c/Å	13.748(10)
α/°	90
β/°	109.51(3)
γ/°	90
V/Å^3	2494(3)
Z	4
ρ_{calc} g/cm^{-3}	1.603
μ/ mm^{-1}	5.492
F(000)	1216.0
Crystal size/ mm^3	0.102 × 0.098 × 0.042
Radiation	MoKα (λ = 0.71073)
2θ range for datacollection/°	3.838 to 51.43
Index ranges	-12 ≤ h ≤ 12, -22 ≤ k ≤ 22, -16 ≤ l ≤ 16
Independent reflections	4783 [R_{int} = 0.1374, R_{sigma} = 0.0633]
Data/restraints/parameters	4738/0/262
Goodness-of-fit on F^2	1.034
R [I>=2θ (I)] (R1, wR2)	R_1 = 0.0384, wR_2 = 0.0812
R (all data) (R1, wR2)	R_1 = 0.0658, wR_2 = 0.0914
Largest diff. peak/hole / (e Å^{-3})	1.60/-1.45

$R1 = \Sigma \, ||F_o|-|F_c|| \, / \, \Sigma \, |F_o|$; $wR2 = [\Sigma(w(F_o^2 - F_c^2)^2) / \Sigma \, w(F_o^2)^2]^{1/2}$

References:

[1] A. Abiko. *Org. Synth*. **2002**, *79*, 103.

[2] Clapson, M. L.; Sharma, H.; Zurakowski, J. A.; Drover, M. W. *Chem. Eur. J.* **2023**, *29*, e202203763.

[3] Neese, F. Software Update: The ORCA Program – Version 5.0. *WIREs Comput. Mol. Sci.* **2022**, 12, e1606.

[4] a) S. Grimme, S. Ehrlich, L. Goerigk, *J. Comput. Chem.* **2011**, 32, 1456; b) S. Grimme, J. Antony, S. Ehrlich, H. Krieg, *J. Chem. Phys.* **2010**, 132, 154104; c) F. Weigend, R. Ahlrichs, *Phys. Chem. Chem. Phys.* **2005**, 7, 3297.

[5] F. Weigend, *Phys. Chem. Chem. Phys.* **2006**, 8, 1057.

[6] a) C. Riplinger, P. Pinski, U. Becker, E.F. Valeeve, F. Neese, *J. Chem. Phys.* **2016**, 144, 024109; b) C. Riplinger, B. Sandhoefer, A. Hansen, F. Neese, *J. Chem. Phys.* **2013**, 139, 134101; c) C. Riplinger, F. Neese, *J. Chem. Phys.* **2013**, 138, 034106.

[7] A. Hellweg, C. Hattig, S. Hofener, W. Klopper, *Theor. Chim. Acta* **1990**, 77, 123.

[8] a) G. Knizia, J.E.M.N. Klein, *Angew. Chem. Int. Ed.* **2015**, 54, 5518; b) G. Knizia, *J. Chem. Theory Comput.* **2013**, 9, 4834.

[9] Bruker (2016). APEX3, SAINT and SADABS. Bruker AXS Inc., Madison, Wisconsin, USA.

[10] L. Krause, R. Herbst-Irmer, G. M. Sheldrick, and D. Stalke, *J. Appl. Cryst.* **2015**, *48*, 3-10.

[11] XDS2SAD, G. M. Sheldrick, **2008**, University of Gottingen, Germany.

[12] a) XPREP, **2014**, Bruker AXS Inc., Madison, Wisconsin, USA. b) XPREP Version 2008, G. M. Sheldrick, 2008 Bruker AXS Inc., Madison, Wisconsin, USA.

[13] Bruker-AXS, SAINT version 2013.8, **2013**, Bruker-AXS, Madison, WI 53711, USA

[14] Bruker-AXS, SADABS version 2012.1, **2012**, Bruker-AXS, Madison, WI 53711, USA

[15] A. L. Spek, *Acta Cryst*. **2009**, *D65*, 148.